Aus dem Department für Diagnostische Labormedizin der
Universität Tübingen

Institut für Pathologie und Neuropathologie
Abteilung Allgemeine und Molekulare Pathologie und
Pathologische Anatomie

AURKA and SRC alterations in neuroendocrine tumors of the small intestine

**Inaugural-Dissertation
zur Erlangung des Doktorgrades
der Medizin**

**der Medizinischen Fakultät
der Eberhard Karls Universität
zu Tübingen**

vorgelegt von

Kalmutzki geb. Kammerlocher, Paulina

2019

Dekan: Professor Dr. I. B. Autenrieth
1. Berichterstatter: Professor Dr. B. Sipos
2. Berichterstatter: Professor Dr. M. Bitzer

Tag der Disputation: 29.08.2018

Table of Contents

LIST OF FIGURES **5**

LIST OF TABLES **6**

ABBREVIATIONS **7**

1. INTRODUCTION **12**

1.1. Neuroendocrine tumors **12**

1.2. Neuroendocrine tumors of the small intestine **14**
1.2.1. Epidemiology 14
1.2.2. Characteristics 15
1.2.3. Clinical appearance and diagnosis 19
1.2.4. Therapy and prognosis 22
1.2.5. Findings of recent studies 23

1.3. AURKA **27**

1.4. SRC **30**

1.5. Aim of the thesis **34**

2. MATERIAL AND METHODS **36**

2.1. Patients and samples **36**

2.2. Tissue microarray **36**

2.3. Chemicals and equipment **37**

2.4. Fluorescence *in situ* hybridization **40**

2.5. Immunohistochemistry **44**

2.6. Statistical analysis **49**

3. RESULTS **50**

3.1. Patient and tumor specifications **50**

3.2. *AURKA* signals determined by fluorescence *in situ* hybridization **50**
3.2.1. *AURKA* signal count 50
3.2.2. Comparison of *AURKA* copy number gains to the findings of Banck *et al.* 54
3.2.3. Relationship between *AURKA* copy number gains and chromosome 18 54
3.2.4. Influence of *AURKA* copy number gains on tumor stage 54
3.2.5. Correlation of *AURKA* copy number gains and survival 56

3.3. AURKA protein expression analyzed by immunohistochemistry 57
3.3.1. AURKA protein expression intensity 57
3.3.2. Correlation of nuclear and cytoplasmic AURKA expression 59
3.3.3. Effect of *AURKA* copy number gains on protein expression 60
3.3.4. Correlation of AURKA expression and tumor progress 60

3.4. *SRC* signals determined by fluorescence *in situ* hybridization 60
3.4.1. *SRC* signal count 60
3.4.2. Comparison of *SRC* copy number gains to the findings of Banck *et al.* 63
3.4.3. Relationship between *SRC* copy number gains and chromosome 18 63
3.4.4. Influence of *SRC* copy number gains on tumor stage 63
3.4.5. Correlation of *SRC* copy number gains and survival 65

3.5. SRC protein expression analyzed by immunohistochemistry 66
3.5.1. SRC protein expression intensity 66
3.5.2. Effect of *SRC* copy number gains on protein expression 69
3.5.3. Correlation of SRC expression and tumor progress 69

4. DISCUSSION 70

5. SUMMARY 75

6. ZUSAMMENFASSUNG 77

7. REFERENCES 79

8. ERKLÄRUNG ZUM EIGENANTEIL DER DISSERTATIONSSCHRIFT 86

ACKNOWLEDGEMENTS 87

List of Figures

Figure 1. Localizations of NETs in the human body. 12
Figure 2. EC cells in the intestinal mucosa. 15
Figure 3. Macroscopic appearance of an ileal NET. 17
Figure 4. Histology of digestive NETs. 17
Figure 5. Contrast-enhanced CT of an ileal NET 21
Figure 6. Axial MRI of a hepatic NET metastasis. 21
Figure 7. Frequency of chromosomal aberrations in gastrointestinal NETs. 24
Figure 8. Quantity of chromosomal alterations in SI-NETs. 25
Figure 9. Centrosome and spindle organization during mitosis. 29
Figure 10. Simplified examples of SRC-mediated signal transduction pathways. 32
Figure 11. Fluorescence *in situ* hybridization technique 42
Figure 12. Immunohistochemical staining methods. 45
Figure 13. Definiens Tissue Studio 2.3.0. workflow. 48
Figure 14. *AURKA* signals (red) visualized by FISH, magnification 1000x. 52
Figure 15. *AURKA* copy number variations grouped into primary tumor and metastases. 53
Figure 16. *AURKA* copy number gains matching UICC stage cluster. 56
Figure 17. Kaplan-Meier survival curves of clinical cases with and without *AURKA* amplifications. 57
Figure 18. Immunohistochemical AURKA staining of a representative SI-NET tissue, magnification 400x 58
Figure 19. Nuclear (nc) and cytoplasmic (cp) AURKA protein expression in primary tumors (P), lymph node metastases (LN) and distant metastases (DM). 59
Figure 20. *SRC* signals (red) displayed by FISH, magnification 1000x. 61
Figure 21. *SRC* copy number variations in primary tumors and metastases. 62
Figure 22. *SRC* copy number variations matching single UICC stages. 65
Figure 23. *SRC* copy number variations matching clustered UICC stages. 65
Figure 24. Overall survival represented by Kaplan-Meier curves with and without *SRC* amplifications. 66
Figure 25. Immunohistochemical SRC staining of an exemplary SI-NET tissue, magnification 400x 67
Figure 26. SRC protein expression based on the Remmele IRS in primary tumors (P), lymph node metastases (LN) and distant metastases (DM). 68
Figure 27. Dichotomic distribution of SRC protein levels in primary tumors (P), lymph node metastases (LN) and distant metastases (DM). 68

List of Tables

Table 1. WHO classification and histopathological grading of NETs of the digestive system..... 16
Table 2. UICC TNM (7th edition) clinical classification of NETs of the small intestine. . 18
Table 3. UICC stage grouping corresponding to TNM criteria of non-appendiceal gastrointestinal NETs. 19
Table 4. Chemicals..... 37
Table 5. Buffers 38
Table 6. Consumable supplies..... 38
Table 7. Equipment 39
Table 8. Antibodies / Probes 40
Table 9. Software 40
Table 10. Percentage of *AURKA* copy number variations determined by FISH. 53
Table 11. *AURKA* copy number gains separated into UICC stages. 55
Table 12. Nuclear (nc) and cytoplasmic (cp) AURKA protein expression..... 58
Table 13. *SRC* copy number variations determined by FISH. 62
Table 14. *SRC* copy number variations in primary tumors and in all clinical cases grouped by tumor stage. 64
Table 15. SRC protein expression. 67

Abbreviations

5-HIAA	5-Hydroxyindoleacetic acid
AKT (1)	Akt serine threonine kinase (1)
ALT	Alternative lengthening of telomeres
APC / C	Anaphase-promoting complex / cyclosome
APUD	Amine precursor uptake and decarboxylation
ATRX	Alpha thalassemia / Mental retardation syndrome X-linked
AURKA	Aurora A serine / threonine kinase
AURKB	Aurora B serine / threonine kinase
AURKC	Aurora C serine / threonine kinase
BCR-ABL	Oncogenic protein product of *BCR* (breakpoint cluster region) and *ABL* (Abelson murine leukemia viral oncogene homolog 1) fusion
BLK	Tyrosine kinase Blk
bp	Base pairs
c-SRC	Cellular Src tyrosine kinase
CAM	Cell adhesion molecule
CDKN1B	Cyclin dependent kinase inhibitor 1B
CEN	Centromere
CGH	Comparative genomic hybridization
CHD	Carcinoid heart disease
COX2	Cyclooxygenase 2
CSK	C-terminal Src kinase
CT	Computed tomography
DAXX	Death domain associated protein
DCC	Deleted in colorectal cancer
DM	Distant metastasis
DNA	Deoxyribonucleic acid

DOPA	Dihydroxyphenylalanine
DOTA	1,4,7,10-Tetraazacyclododecane-1,4,7,10-tetraacetic acid (chelator)
DOTATATE	DOTA-Tyr(3)-octreotate (radiolabeled somatostatin analog)
DOTATOC	DOTA-Phe(1)-Tyr(3))octreotid (radiolabeled somatostatin analog)
EC	Enterochromaffin
EGF(R)	Epidermal growth factor (receptor)
ENETS	European Neuroendocrine Tumor Society
F	Fluorine
FAK	Focal adhesion kinase
Fc	Fragment crystallizable region
FDA	Food and Drug Administration
FDG	Fluorodeoxyglucose
FFPE	Formalin-fixed paraffin-embedded
FGF(R2)	Fibroblast growth factor (receptor 2)
FGR	Tyrosine kinase Fgr
FISH	Fluorescence *in situ* hybridization
FITC	Fluorescein isothiocyanate
FOS	Fos proto-oncogene
FYN	Tyrosine kinase Fyn
G1 phase	First growth phase of the cell cycle
G2 phase	Second growth phase of the cell cycle
Ga	Gallium
GEP-NET	Neuroendocrine tumor of the gastroenteropancreatic system
HCK	Tyrosine kinase Hck
H&E	Hematoxylin and eosin
HER1	Human epidermal growth factor receptor 1
HER2	Human epidermal growth factor receptor 2

HIF-1	Hypoxia-inducible factor-1
HPF	High power field
IHC	Immunohistochemistry
In	Indium
kDa	Kilodalton
Ki-67	Proliferation marker antigen Ki-67
L	Enteroglucagon
LCK	Tyrosine kinase Lck
LN	Lymph node metastasis
Lu	Lutetium
LYN	Tyrosine kinase Lyn
M phase	Mitotic phase of the cell cycle
MAPK	Mitogen-activated protein kinase
MEN1	Multiple endocrine neoplasia 1
MRI	Magnetic resonance imaging
(m)RNA	(Messenger) ribonucleic acid
mTOR	Mammalian target of rapamycin
MYC	Myelocytomatosis transcription factor
N	Neurotensin
NEC	Neuroendocrine carcinoma
NET	Neuroendocrine tumor
NF-κB	Nuclear factor κ B transcription factor
NF1	Neurofibromatosis type 1
NFKBIA	Nuclear factor κ B inhibitor α
NGS	Next generation sequencing
p-	Phosphorylated
P	Primary tumor

p190 Rho GAP	p190 Rho GTPase activating protein
p53	Tumor suppressor protein p53
PCR	Polymerase chain reaction
PET	Positron emission tomography
PDGF(R)	Platelet derived growth factor (receptor)
PI3K	Phosphatidylinositol 3 kinase
PKA	Protein kinase A
PP1	Protein phosphatase 1
PPRT	Peptide receptor radionuclide therapy
R0	No residual tumor
RALA	Ras like proto-oncogene A
RANK	Receptor activator of nuclear factor κ B
RAS	Rat sarcoma protein family
RFA	Radiofrequency ablation
S phase	Synthesis phase of the cell cycle
SEER	Surveillance, Epidemiology and End Results
SI-NET	Neuroendocrine tumor of the small intestine
SIRT	Selective internal radiation therapy
SRC	Src tyrosine kinase
SSA	Somatostatin analogs
SSR	Somatostatin receptor
SSRS	Somatostatin receptor scintigraphy
STAT (3 / 5)	Signal transducer and activator of transcription (3 / 5)
T1	Magnetic resonance imaging sequence based on longitudinal (spin-lattice) relaxation
T2	Magnetic resonance imaging sequence based on transverse (spin-spin) relaxation
TA(C)E	Transarterial (chemo)embolization

Thr	Threonine
TMA	Tissue microarray
TNM	Classification system considering the extent of primary tumor, lymph node metastases and distant metastases
TPX2	Target protein for xenopus kinesin-like protein 2
TSC1	Tuberous sclerosis complex 1
Tyr	Tyrosine
UICC	Union for International Cancer Control
v-SRC	Viral Src tyrosine kinase
VEGF	Vascular endothelial growth factor
VHL	Von Hippel-Lindau
WES	Whole exome sequencing
WHO	World Health Organization
YAC	Yeast artificial chromosome
YES	Tyrosine kinase Yes
YRK	Tyrosine kinase Yrk

1. Introduction

1.1. Neuroendocrine tumors

Neuroendocrine tumors (NETs) are neoplastic lesions originating from progenitor cells that resemble both neurons and endocrine cells. They share common structural features (specific antigens) and functional characteristics (secretory vesicles) with both cell types. Due to their ability to produce hormones and neurotransmitters, these cells are referred to as neuroendocrine cells. Since neuroendocrine tissue is organized in islets within endocrine glands or dispersed as diffuse endocrine system throughout the whole body, NETs can arise from various organs (Figure 1).

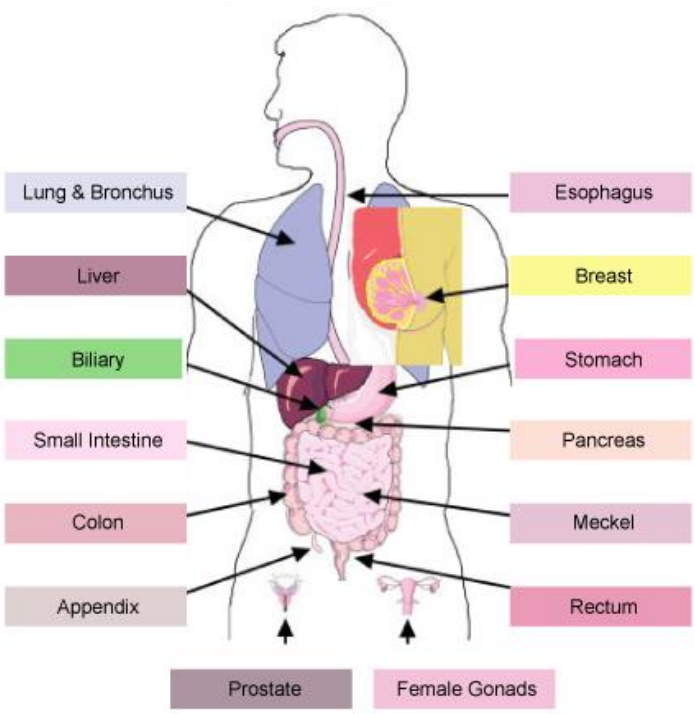

Figure 1. Localizations of NETs in the human body. Modified according to ref. [1].

Depending on their embryological development, NETs are subdivided into foregut, midgut, hindgut and extraintestinal derivates. Most commonly they emerge from the gastrointestinal system followed by the bronchopulmonary

system.[2] Yet, some have also been noticed in the hepatobiliary and urogenital system and may arise from (extra) adrenal paraganglia, nerve plexuses, the breast and the skin. Based on the actual organ site, there is a large variety of clinical progression and outcome. While sporadic NETs of specific locations rather develop at an older age, NETs of other sites occur in younger people, particularly those associated with inherited syndromes like neurofibromatosis type 1 (NF1), multiple endocrine neoplasia type 1 (MEN1), von Hippel-Lindau disease (VHL) or tuberous sclerosis (TSC1).[3]

NETs are separated into two species dependent on their secretory activity: (1) functionally active tumors which release diverse hormones (polypeptides such as gastrin and biogenic amines like serotonin), neurotransmitters, mediators, growth factors and cytokines corresponding to their tissue of origin and (2) functionally inactive tumors. Although both groups produce and store secretory products, functionally active NETs are characterized by excessive hormone release. This, in turn, can lead to substance-specific symptoms, for example the Zollinger-Ellison syndrome in case of gastrinoma.

The US National Cancer Institute's Surveillance, Epidemiology and End Results (SEER) study pointed out that with a rising incidence from 1.09/100,000 in the 1970s to 5.25/100,000 in 2004 this comparatively rare tumor entity has grown remarkably in importance over the last decades. A significant part of the diagnosed NETs (20-50%, depending on tumor differentiation) presented contemporaneous distant metastases, which reduced the median survival from 223 to 33 months in case of well to moderately and from 34 to 5 months in case of poorly differentiated NETs, respectively.[4]

There have been many different nomenclature and classification attempts in order to define NETs but they were inconsistent regarding the tumor precursor cells.[5]

Despite these heterogeneous tumors being largely grouped together as one entity, an early and precise detection of the tumor with its organ of origin, grade and stage are crucial for the prognosis and survival. In order to standardize the diagnosis and treatment conditions, the World Health Organization (WHO) has

set a histologically based grading and classification system in 2010. The grading criteria, however, vary among the different organs. Regarding invasiveness and capacity to spread, all NETs are potentially malignant tumors. Considering the extent of the primary tumor (T), lymph node metastases (N) and distant metastases (M), they are staged by the TNM classification system developed by the Union for International Cancer Control (UICC). The strongly variable prognostic value among this heterogeneous tumor entity and the need of a proper patient stratification resulted in the establishment of separate TNM classifications for different localizations. As largest subgroup, NETs of the gastroenteropancreatic system (GEP-NETs, including gastric, intestinal and pancreatic NETs) have been classified separately by the European Neuroendocrine Tumor Society (ENETS) prior to the UICC categorization.

1.2. Neuroendocrine tumors of the small intestine

1.2.1. Epidemiology

NETs of the small intestine (SI-NETs) have their origin in the diffuse endocrine system of the duodenum, jejunum and most commonly of the ileum. With 28.5%, SI-NETs represent a major part of all gastrointestinal NETs.[2] Although in general they are rare, with an incidence of approximately 1/100,000 cases, there tumors are the most frequent malignant tumor of the small intestine with an increasing prevalence.[6]

Not only have the improvements in classification and diagnostics given rise to the step-up in incidence. The influence of alimentary factors is being discussed as well.[4] The gender and race distribution varies among different countries. While the male-to-female ratio is fairly balanced in total, the African American ethnicity is more affected than other ethnic groups.[4,7] SI-NETs predominantly emerge in patients between 60 and 70 years and despite the majority occurring sporadically, there have been case reports of familial association.[8,9]

1.2.2. Characteristics

Most frequently, SI-NETs evolve from enterochromaffin (EC) cells located in the basal mucosal epithelia disseminated throughout the intestinal system (Figure 2). Their function is to regulate the digestive activity by paracrine secretion of serotonin and bioactive mediators. Stored in secretory granules these hormones give EC cells a fine-grain appearance. Beyond that, there are more neuroendocrine cells of the small intestine, such as the enteroglucagon (L) cells which balance the blood sugar level, or neurotensin (N) cells adjusting acidity and motility. However, tumors of these origins are extremely rare.

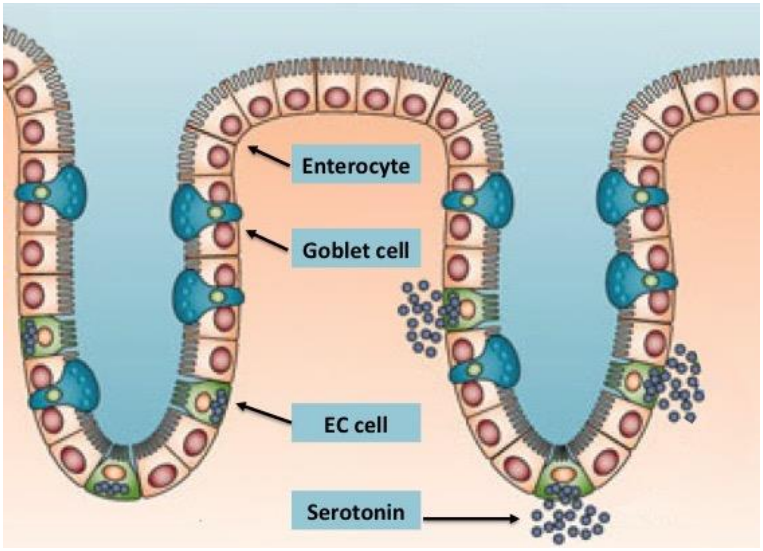

Figure 2. EC cells in the intestinal mucosa. EC cells (green) in the intestinal crypts store and release serotonin granules (dark blue). Modified according to ref. [10].

Analogous to the neuroendocrine cells of the gastrointestinal system that in total represent the largest endocrine organ, SI-NETs express nonspecific neuroendocrine biomarkers such as chromogranin A, synaptophysin and neuron-specific enolase. In addition, they exhibit type-specific markers like somatostatin receptors (SSR) on their cell surface, or their synthesis products. With regard to their histological appearance, there are four potential growth patterns: (1) nodular nests, (2) trabecular structure, (3) tubular, acinar or rosette like and (4) atypical differentiation.[11]

As a subgroup of GEP-NETs, neuroendocrine neoplasms of the small intestine are graded by the WHO (2010) classification considering their differentiation and proliferation rate into low grade (G1: Ki-67 proliferation index ≤ 2%, < 2 mitoses / 10 high power fields [HPF] with a size of 2 mm^2 each), intermediate grade (G2: Ki-67 index 3-20%, 2 - 20 mitoses / 10 HPF) well differentiated neuroendocrine tumors and high grade (G3: Ki-67 index > 20%, > 20 mitoses / 10 HPF) poorly differentiated neuroendocrine carcinomas (Table 1).[12]

Table 1. WHO classification and histopathological grading of NETs of the digestive system.

Classification	**Grade**	**Mitotic count (per 10 HPF)**	**Ki-67 index**
NET	G1 (low grade)	<2	≤2 %
NET	G2 (intermediate grade)	2-20	3-20%
NEC	G3 (high grade)	>20	>20%

SI-NETs generally grow slowly (mostly graded G1/G2) and reach an average size of a few centimeters. The macroscopic appearance of an ileal NET is depicted in Figure 3. Two different histologic growth patterns of digestive NETs are demonstrated by hematoxylin and eosin (H&E) stainings in Figure 4.

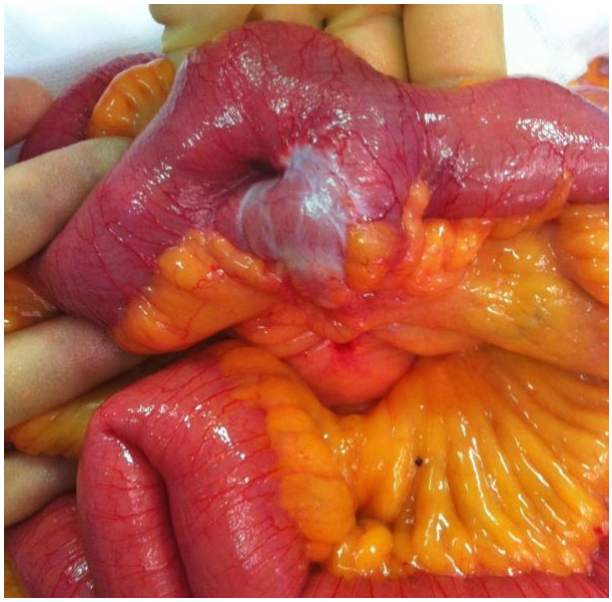

Figure 3. Macroscopic appearance of an ileal NET. The tumor stands out as a whitish, fibrotic mass. Retrieved from: http://www.hpbsurgery.co.za/intestinal-tumours.php. Date accessed: 06/04/2017

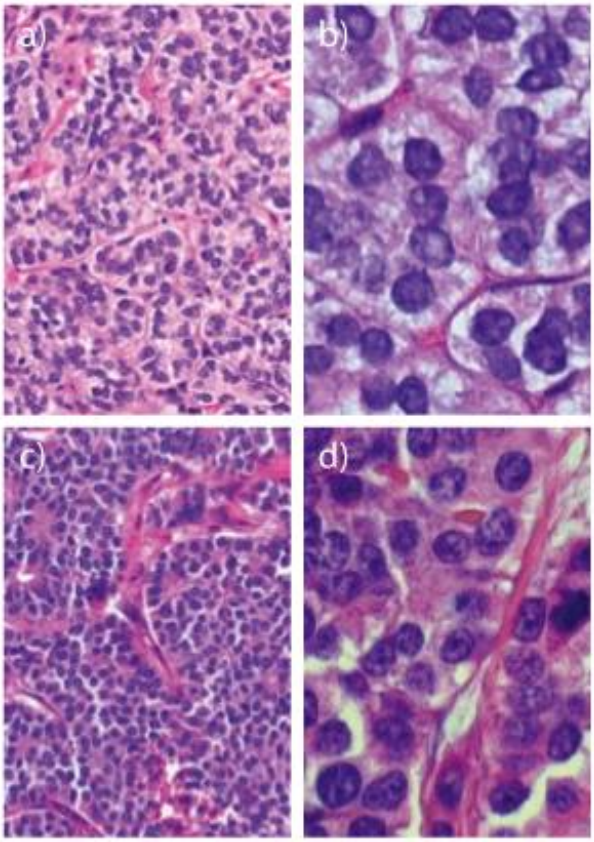

Figure 4. Histology of digestive NETs. H&E stainings. a) Trabecular / solid / gyriform patterns with b) minor cellular atypia are characteristic of G1 tumors. c) Consolidated trabecular structures with d) moderate atypia are characteristic of G2 tumors.[13]

Once they expand from the tela submucosa to the tunica muscularis mucosae SI-NETs are likely to spread out lymph node or distant metastases, which is classified by the TNM system of neuroendocrine tumors of the small intestine (Table 2). According to the particular parameters for the extent of the primary tumor, lymph node and distant metastases, SI-NETs are grouped into different stages, as demonstrated in Table 3.

Table 2. UICC TNM (7th edition) clinical classification of NETs of the small intestine.

T	**Primary tumor: add (m) for multiple tumors**
TX	Primary tumor cannot be assessed
T0	No evidence of primary tumor
T1	Tumor invades lamina propria or submucosa and is ≤ 1 cm in size
T2	Tumor invades muscularis propria or is > 1 cm in size
T3	Jejunal or ileal tumor invades subserosa Ampullary or duodenal tumor invades pancreas or retroperitoneum
T4	Tumor perforates visceral peritoneum (serosa) or invades other organs or adjacent structures
N	**Regional lymph nodes**
NX	Regional lymph nodes cannot be assessed
N0	No regional lymph node metastasis
N1	Regional lymph node metastasis
M	**Distant metastasis**
M0	No distant metastasis
M1	Distant metastasis

Table 3. UICC stage grouping corresponding to TNM criteria of non-appendiceal gastrointestinal NETs.

Stage	**Corresponding TNM criteria**		
Stage I	T1	N0	M0
Stage IIA	T2	N0	M0
Stage IIB	T3	N0	M0
Stage IIIA	T4	N0	M0
Stage IIIB	Any T	N1	M0
Stage IV	Any T	Any N	M1

Since metastases are often considered a life-limiting factor, SI-NETs show a high potential for malignancy in contrast to the mostly benign NETs of the stomach and of the appendix.[14]

1.2.3. Clinical appearance and diagnosis

Unlike other types of NETs, SI-NETs are not part of congenital syndromes and therefore, do not show specific symptoms. Since most of them are small, slowly growing and functionally inactive, they tend to be diagnosed late, sometimes even coincidently during other examinations or surgery.

Usually this tumor manifests very late with unspecific problems like pain, nausea and vomiting due to the bulk expansion. In contrast, serotonin as main secretory substance has various concealed effects on the environment of SI-NETs. It stimulates the proliferation of fibroblasts, endothelial cells and induces smooth muscle growth.[15] However, only in less than 10% of the patients and only in case of functional activity, excessive secretion of serotonin or mediators like kallikrein, tachykinins or prostaglandins can provoke a particular symptom complex denoted as carcinoid syndrome.[16] It not only includes local effects of inappropriate serotonin and growth factor release such as desmoplastic reaction, intestinal obstruction and ischemia but more importantly has a systemic impact. The most common systemic manifestations are flushing, diarrhea, abdominal pain, palpitations, endocardial fibrosis, valvular heart disease and heart failure (referred to as carcinoid heart disease CHD). Occasionally symptoms like

bronchial constriction and spasm, wheeze, teleangiectasia, arthritis and pellagra occur.[3] If enhanced by stress or medical procedures facilitating mediator release (such as intraoperative mechanical stimulation), carcinoid syndrome can devolve into a life-threatening crisis with signs of medical shock.[16]

A common characteristic of SI-NETs is the extensive metastatic spread leading to lymph node metastases in 60% of the patients at the time of diagnosis and to metastases in general in more than 70% over the course of time, regularly gaining a multiple of the primary tumor's size.[3,17] As the most affected organ by distant metastases, the liver becomes functionally restricted and fails to inactivate circulating vasoactive hormones and mediators. Insufficient metabolization explains why the few specific symptoms of SI-NETs mainly present in patients with advanced, metastatic SI-NETs.

For diagnostic purposes, medical history and physical examination usually are not informative. Laboratory findings may detect an excess of secretory markers (serotonin, neurokinin A, neuropeptide K, substance P) and biomarkers for CHD (natriuretic peptides) in blood serum or urinary 5-hydroxyindoleacetic acid (5-HIAA) as metabolic product of serotonin.[11,17]

Over the last years, diagnostic imaging has become more and more important for identifying the tumor and metastases, choosing the right treatment, monitoring its response and for follow-ups. This is due to two factors: first, diagnostic radiology came up with a variety of highly specific visualization methods; second, the advance in image resolution has remarkably improved the detection rate of these mostly small tumors. Nevertheless, none of the available imaging techniques achieve to gather all required information at once, making multimodal imaging necessary. Giving a rough insight into the gastrointestinal tract and the possibility to navigate a subsequent biopsy if needed, transabdominal sonography is a good starting point for further investigations. Especially power Doppler sonography is used to visualize the vascularization of the tumor mass and, in appropriate cases, enteroscopy or endocapsule imaging provide a higher resolution image of the suspicious segment. Conventional (contrast-enhanced) computed tomography (CT), magnetic resonance imaging (MRI), ^{111}In-Octreotide somatostatin receptor

scintigraphy (SSRS) and ^{68}Ga positron emission tomography (PET) are likewise used for identifying SI-NETs and, once they have been diagnosed, for staging and determining the resectability.[17,18] Figure 5 illustrates a typical contrast-enhanced CT of an ileal NET during the portal venous phase presenting a mesenteric node metastasis (a) and a hepatic metastasis (b). Figure 6 depicts a T1-weighted (a) and T2-weighted (b) MRI sequence of a hepatic NET metastasis.

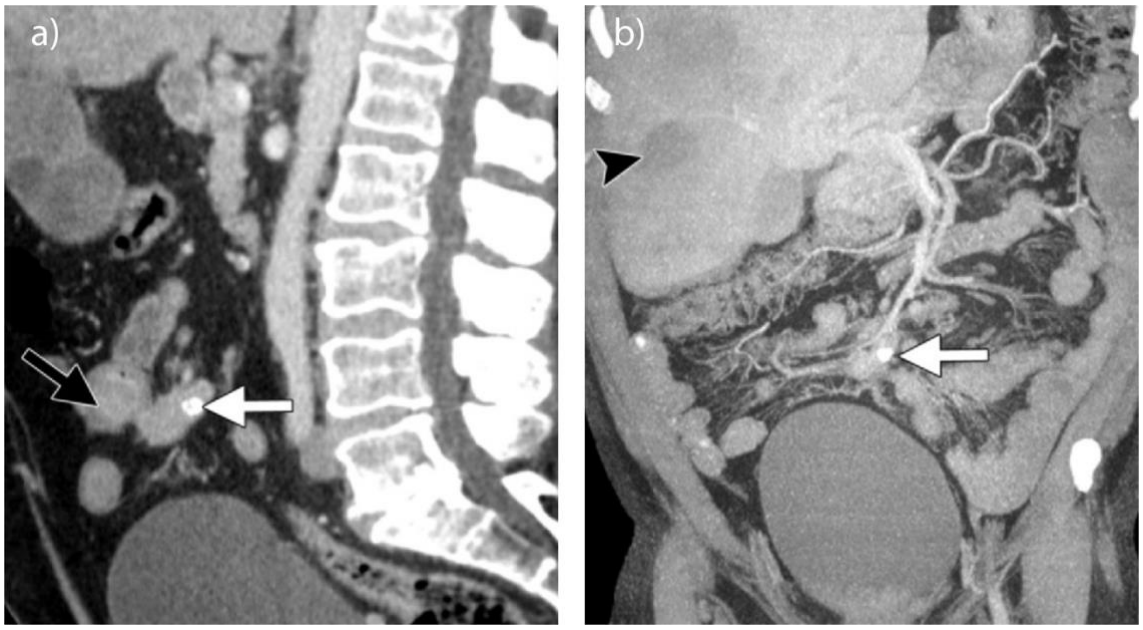

Figure 5. Contrast-enhanced CT of an ileal NET. Portal venous phase imaging. a) Primary tumor in a sagittal layer (black arrow) with calcified mesenteric nodes (white arrow), b) hepatic metastasis in a coronal layer (black arrowhead).[18]

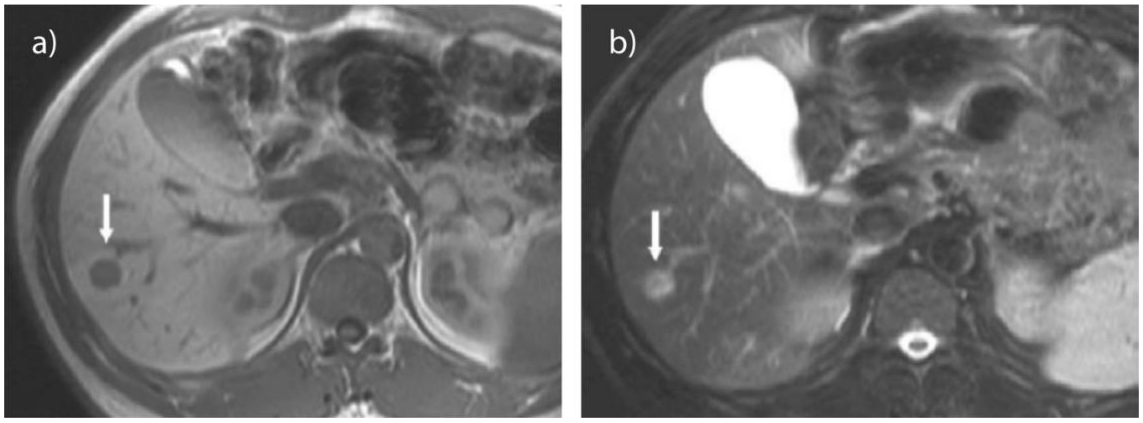

Figure 6. Axial MRI of a hepatic NET metastasis. a) T1-weighted, b) T2-weighted image of the metastatic mass (white arrow).[3]

Further functional imaging techniques aim to display particular features. For example the metabolism of glucose as indicator of a tumor's mitotic rate can be detected by ^{18}F-fluorodeoxyglucose (FDG) PET (generally low in SI-NETs), amine uptake and decarboxylation (characteristic for SI-NETs regardless of functional activity) can be verified by ^{18}F-DOPA PET, and the identification of SSR can be visualized with ^{68}Ga-DOTATOC (radiolabeled SSR ligand) PET/CT giving direction to the therapeutic setting.[18]

1.2.4. Therapy and prognosis

The overall outcome is extremely affected by tumor dissemination at the time of diagnosis that is usually significant because of late and nonspecific clinical manifestation and poor response to standard cancer therapy. This is exemplified by the median survival for localized small bowel NETs of 111 months decreasing to 105 months in case of regional node metastases and to 56 months in case of distant metastases.[4]

Although limited by the extent of tumor spread and the patient's comorbidities, radical surgical resection of primary tumor and metastases is the only way to cure the patient. Thus, surgery intending a R0 situation (no residual tumor mass) is considered first-line therapy. If the tumor is not completely resectable the patient can undergo a multidisciplinary treatment approach consisting of cytoreductive surgery, medication and interventional radiotherapy.

Cytoreductive surgery aims to reduce bulk volume related symptoms. In addition, the response to subsequent treatment can be augmented by removing tumor and metastatic mass (by usually 70-90%) if possible.[19]

The global aim of palliative medication is to decelerate tumor growth, decrease the symptoms of abundant hormones and in doing so improve the quality of life. Interferons such as Interferon-α are established as universal anti-tumor drugs because they stimulate the immune system and thereby support the endogenous control over tumor growth. Even though effective for SI-NETs, they are not tolerated by all patients because of multiple side effects. Another essential therapeutic target for functionally active SI-NETs is somatostatin. This peptide hormone acts as inhibitory counterpart to most of the gastrointestinal hormones,

which pharmacologically can be taken advantage of. Somatostatin analogs (SSAs, binding to somatostatin receptors 1-5) such as Octreotid or Lanreotid have proven to be successful anti-proliferative substances with low side effects. Besides, SSAs are used as preoperative medication preventing the carcinoid crisis.

Complementary to surgery and medication, radiotherapy is a palliative procedure widely used for the elimination of liver metastases. This can be achieved by locally ablative procedures like radiofrequency ablation (RFA), cryotherapy, transarterial (chemo)embolization (TAE / TACE) or radioembolization like selective internal radiation therapy (SIRT). Peptide-receptor radionuclide therapy (PPRT) with radiolabeled SSA (^{90}Y-DOTATOC or ^{177}Lu-DOTATATE) allows for a selective uptake of the β-emitter isotopes by SSR expressing tumor cells limiting the damage of surrounded tissue.[17]

Since cytotoxic chemotherapy is most effective for highly proliferative cancer, it is an option for NECs, but not applicable for the slowly growing NETs due to their lack of response.

Despite improved diagnostic methods and the mentioned treatment trials, the 5 year survival rate of 60% has not changed over the last decades, which points to the necessity of innovative treatment options.[11] Following the first successful substances in diverse studies on individualized GEP-NET immunotherapy like Bevacizumab (monoclonal antibody inhibiting vascular endothelial growth factor VEGF), Sunitinib (multi-targeted tyrosine kinase inhibitor) and Everolimus (mammalian target of rapamycin mTOR inhibitor), inhibitory agents in tumorigenic signal pathways and cell environments are highly demanded.[11] Therefore, however, a greater understanding of the underlying genetics and protein expression has to be attained.

1.2.5. Findings of recent studies

Genetic instability such as chromosome and nucleotide rearrangements has proven to play an important role in carcinogenesis. Defects in DNA damage repair, chromatin remodeling and mitosis / apoptosis regulation are the most

prominent factors to misbalance cell growth and proliferation. The prognosis in general is associated with the amount of karyotypic variations.[20]

Since the molecular etiology of NETs is largely still unknown, recent research has focused on chromosome instability and genomic alterations in established tumor inducing and maintaining pathways. Comparative genomic hybridization (CGH) was the first method used in multiple analyses of numeric chromosomal aberrations in gastrointestinal NETs with loss of chromosome 18 considered a breakthrough discovery.[21-25] Besides, distinct chromosomal gains (4, 5, 19, 20q) were common events in several GEP-NETs. Gains of the long arm of chromosome 20 as the most frequent amplification in foregut NETs (58%) for instance represented a considerable part of midgut NET alterations (36%). On the contrary, some other chromosomes were multiplied by preference in foregut (17p) or midgut (17q, 19p).[22] Figure 7 illustrates the frequency of chromosome abnormalities in GEP-NETs emphasizing loss of chromosome 18 as the most common event.

Figure 7. Frequency of chromosomal aberrations in gastrointestinal NETs. Comparison of highly frequent (bottom) and less frequent events (top).[26]

Loss of heterozygosity of tumor suppressor genes located on chromosome 18 is estimated a major candidate in driving SI-NET tumorigenesis, just as in other gastrointestinal tumor species.[27] Therefore, the working group of Prof. Sipos

analyzed seven tumor suppressor genes located on chromosome 18 in SI-NETs *via* Immunohistochemistry (IHC) and Western Blot revealing a reduced expression of DCC (Deleted in Colorectal Cancer gene) in about 30% of the investigated samples.

The previously identified chromosomal aberrations were confirmed by Banck *et al.* through DNA investigation of 48 patients with SI-NETs by whole exome sequencing (WES), the first genome-wide analysis comprising more than 20,000 genes.[28] Figure 8 compares spotted chromosomal gains (most notably in chromosome 4, 5, 14 and 20) and losses (predominantly chromosome 18).

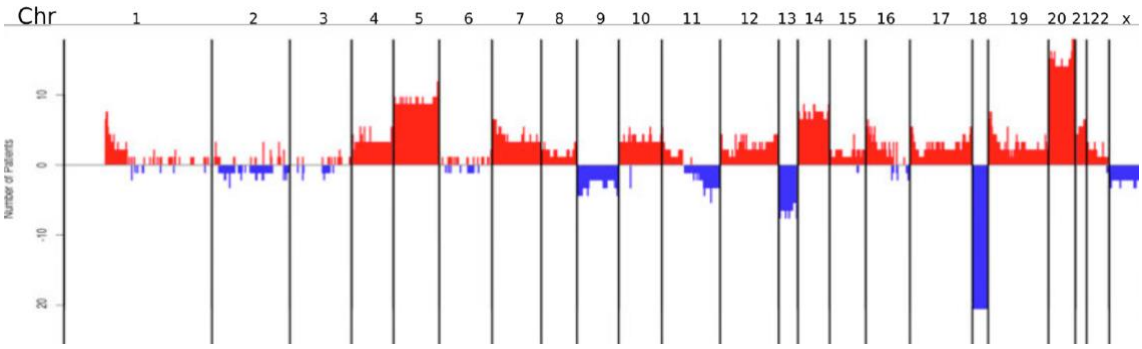

Figure 8. Quantity of chromosomal alterations in SI-NETs. Signal gains (red, above midline) and losses (blue, below midline) detected by whole exome sequencing are displayed for each chromosome separately.[28]

Abnormalities of particular chromosomes (loss of 18q and 11q) have been considered as early events of malignant transformation, whereas other chromosomal alterations (loss of 16q and gain of 4p) predominantly found in metastases seem to be late events and markers of tumor progression.[25] In several cases, copy number gains affected at least chromosome 4 and 20 simultaneously and were almost always correlated with a loss of chromosome 18, whereas chromosome 18 losses in many cases occurred isolated.[29] This confirmed that different mechanisms lead to early and late events, respectively. Also, genetic heterogeneity was seen as indicative of different neoplastic cell populations, which implies multiple molecular pathways driving tumorigenesis in SI-NETs.[30]

At molecular level, Banck *et al.* revealed somatic copy number variations and mutations in several cancer-related signaling pathways. For example, they found alterations in PI3K / AKT / mTOR signaling, which cause apoptosis escape and can immortalize tumor cells. This finding corresponds with positive clinical effects of mTOR-inhibitor Everolimus in other types of GEP-NETs (unlike SI-NETs). Spotted gains in signal associated genes like *EGFR* (Epidermal growth factor receptor), *PDGFR* (Platelet derived growth factor receptor) and mutations in *FGFR2* (Fibroblast growth factor receptor 2) could also explain dysregulations of this pathway.[28]

In addition, copy number gains were detected in proto-oncogenes, most frequently in *SRC* (encoding for Src tyrosine kinase) and its downstream effectors.[28]

Inactivating mutations of *CDKN1B* (encoding for Cyclin dependent kinase inhibitor 1B) and gains in *AURKA* (encoding for Aurora A serine / threonine kinase) are two examples of reported alterations in cell cycle regulators as major source of genetic instability in SI-NETs.[28,29]

The identified genomic alterations in SI-NETs widely vary from other GEP-NETs. Pancreatic NETs, for example, represent the greatest part of NETs associated with inherited syndromes, most commonly MEN1.[31] *MEN1*, a tumor suppressor that represses telomerase activity, is most frequently inactivated in pancreatic NETs. The second most common mutations concern *ATRX / DAXX,* encoding for a chromatin remodeling complex.[32] Inactivation of this complex modifies telomeric chromatin and leads to alternative lengthening of telomeres (ALT). This constitutes an essential mechanism of tumor cell immortality.[33] Moreover, gastrointestinal NETs for their part are based on different molecular conditions than NETs of other provenance. This concerns distribution patterns of chromosomal aberrations; for example the most frequent event in GEP-NETs is loss of chromosome 18, whereas bronchial NETs most of all feature loss of chromosome 11 and chromosome 18 is preserved.[24,34] Beyond, alterations of *MEN1* (located on chromosome 11), seem to be likewise involved in sporadic bronchopulmonary NETs but less likely in gastrointestinal NETs.[35,36] This

assumes that clinical appearance and outcome is determined by different molecular mechanisms. NETs should therefore no longer be seen as one entity.

1.3. AURKA

The human Aurora kinase enzyme family consists of Aurora kinase A, B and C; all nonspecific serine/threonine kinases holding a regulatory function in cellular division. These proteins correspond in the C-terminal position of their catalytic domains but vary in length, subcellular compartment, function and the localization of their encoding genes (*AURKA*, *AURKB*, *AURKC*).

AURKA, encoding for Aurora kinase A is located on the chromosomal region 20q13.2 measuring 22,949 bp. The protein consists of 403 amino acids with a total molecular mass of 45.8 kDa and is expressed in the nucleus, cytosol and centrosome of proliferating cells in many tissues (most notably in brain and the gastrointestinal system). As one of the key mitotic regulators it is highly expressed between the S and M phase and is involved in the centrosome maturation, mitotic entry, microtubule assembly and stabilization of the bipolar spindle apparatus required for correct chromatid segregation, and cytokinesis.

Aurora A activity depends on its expression degree and is terminated by anaphase-promoting complex / cyclosome (APC / C) ubiquitination and proteasome degradation when mitosis is completed.[37] Enzyme activity is temporally controlled by different phosphorylation mechanisms at Thr_{288} including protein kinase A (PKA), whereas phosphorylation can be reversed by protein phosphatase 1 (PP1). It is spatially regulated by auxiliary agents such as TPX2 (Target protein for Xenopus kinesin-like protein 2) relocating the protein to the spindle and centrosome and potentiating the enzyme capacity *via* autophosphorylation and PP1 antagonism.[38]

First observed in breast and colorectal malignancies, *AURKA* amplification and protein overexpression has been found in many cancer types, such as ovarian, cervical or prostate tumors and subsequently was demonstrated to cause *in vitro* and *in vivo* malignant transformation in human and rodent cell lines.[39,40] The enhanced expression, however, is only partially ascribed to gene amplification.

This is exemplified by a CGH study on gastric cancer, in which AURKA overexpression was identified in 50% of the cases, whereas only 5% showed gene amplification as well.[41] Presenting with regular copy numbers it can likewise be generated by intensified transcription, aberrant activation (for example by phosphorylation site mutations) or interactions with regulatory genes or proteins like PP1.[42] Intensified interactions which already existed and newly acquired ones could both account for the nuclear and cytoplasmic excess of Aurora A during the entire cell cycle in cancer cells.[43]

Excessive Aurora A activity intensifies the G1 / S cell cycle shift by up-regulation of cyclins and cyclin dependent kinases; firstly, by transcript polyadenylation and secondly, by enforced activation of polo-like kinase 1 and its downstream proteins.[43-45] Moreover, Aurora kinases are suspected to overregulate H3 histone phosphorylation conditioning the mitotic entry.[37] Elevated Aurora kinase A levels also assist in skipping mitotic spindle checkpoints which monitor the correct chromosomal alignment.[46] In normal cells, a feedback system between Aurora A and the tumor suppressor p53 (most important damage-related mediator of apoptosis) keeps cell growth and death in balance. If overexpressed, Aurora A defies this control mechanism by phosphorylating and thereby inactivating p53.[47] Cells with poorly aligned chromosomes are thus still able to multiply.

In summary, overexpression of Aurora kinase A has been observed to accelerate cell proliferation with amplified centrosomes, irregular spindles, chromatid mis-segregation, failure in cytokinesis and decreased apoptosis, as illustrated in Figure 9.[44] This explains the oncogene-like function of *AURKA* in carcinogenesis and also the variety of chromosomal aberrations in corresponding malignancies.[26]

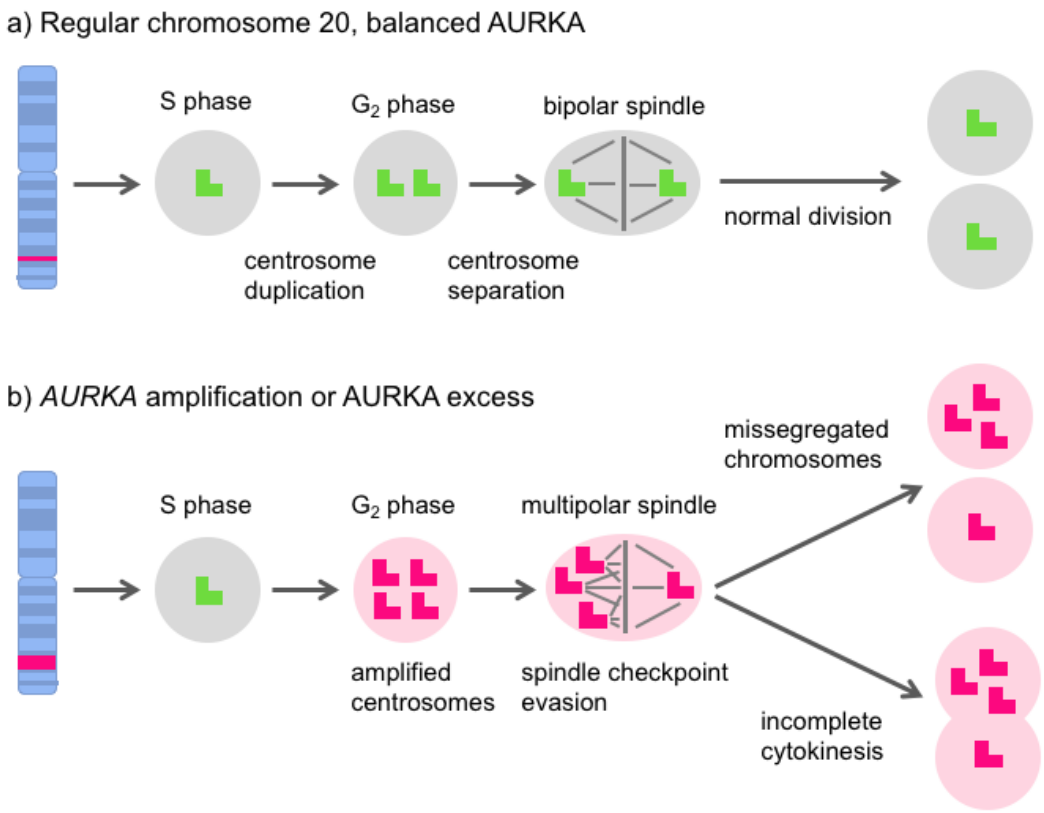

Figure 9. Centrosome and spindle organization during mitosis. a) Cells with balanced AURKA levels and normal chromosome 20 divide regularly (green). b) Cells with *AURKA* amplification or increased protein activity with disrupted mitotic spindles result in chromosomal missegregation or aneuploidy (pink). Modified according to ref. [38,45].

Increased Aurora A expression additionally has two detrimental consequences. First, it interacts with cancer-driving proteins: Aurora A-induced phosphorylation up-regulates NF-κB (nuclear factor κ B) by degradation of NF-κB inhibitor α (NFKBIA), it activates AKT1 and it stimulates the RAS pathway *via* Ras like proto-oncogene A (RALA), which jointly enhances cell survival, proliferation and motility.[48] Second, it cuts cancer treatment response by inducing resistance to tubulin-targeting chemotherapy like Paclitaxel and reducing apoptotic response to Cisplatin, both of which are used for many of the previously mentioned tumor types.[46,47] Therefore, *AURKA* amplification or overexpression could serve as predictive biomarker. But most importantly, this fact points out the attractiveness of simultaneously stopping tumor progression and improving overall treatment results with appropriate enzyme inhibitors.

Inspired by the success of state-of-the-art immunotherapy, multiple Aurora kinase inhibitors have been designed and are currently tested in preclinical and clinical trials. For unresectable, previously unmanageable SI-NETs, the phase II candidate drugs Alisertib (MLN8237) and Danusertib (PHA-739358) open up new treatment perspectives.[49] *In vivo* experiments of human GEP-NET cell lines expressing Aurora kinase A demonstrated tumor growth reduction and lower levels of biomarkers after Danusertib application in a xenograft mouse model. These results were confirmed by a cell-cycle arrest *in vitro*.[50] With limited adverse drug effects (neutropenia) this target therapy is generally well tolerated.

1.4. SRC

SRC is part of the first identified proto-oncogenes. It was discovered by Michael Bishop and Harold Varmus, who were jointly awarded the Nobel Prize in Physiology or Medicine in 1989 for their findings on the origin and impact of oncogenes.[51] *SRC* encodes for non-receptor tyrosine kinase SRC, head of the Src kinase family including other structurally resembling proteins (FYN, YES, YRK, BLK, FGR, HCK, LCK and LYN). First isolated as viral *SRC* mutant (v-*SRC*) from the Rous sarcoma virus (avian retrovirus) *SRC*'s provenance has been identified as cellular gene in vertebrates (c-*SRC*, in short: *SRC*).[52]

SRC is mapped to the chromosomal region 20q11.23 and has a size of 61,366 bp. The 59.8 kDa protein composed of 536 amino acids is characterized by cytoplasmic and membranous expression in neurons, thrombocytes and proliferating cells of many tissues (predominantly in adrenal glands, the bronchial system and reproductive organs). [53,54]

Enzyme activity is initiated during the G_2/M cell cycle transition by phosphorylation at Tyr_{416} (either autophosphorylation or *via* intramolecular conformational changes) subsequent to activation of different receptors. The most important receptor classes in this context are receptor tyrosine kinases (mainly EGFR and PDGFR), cytokine receptors like Receptor Activator of Nuclear Factor κ B (RANK) and integrins (mediators of cell-cell and cell-matrix contacts). Moreover, SRC is regulated by cell adhesion molecules (CAMs), G-

protein-coupled receptors (such as β-adrenergic receptors) and steroid receptors (for example by the progesterone receptor).[55] SRC and its activating receptors underlie remarkable mutual regulation.[56] Therefore, it represents an interface between extracellular signals and cellular signal transduction pathways.

Once activated, it phosphorylates cellular proteins at specific tyrosine residues. These proteins consequently interact with effectors of diverse biological procedures, most importantly gene transcription, cell differentiation, proliferation, survival, cell-cell adhesion, migration and angiogenesis.[57] Figure 10 exemplifies SRC's interactive network highlighting the complexity of cross-talking pathways. All of these physiological functions can contribute to malignant transformation and metastatic spread if running out of control. In contrast to the constitutively active viral oncogene, cellular Src kinase can be inhibited *via* phosphorylation at Tyr_{527} by C-terminal Src kinase (CSK). Thus, *SRC* is referred to as a proto-oncogene.[58]

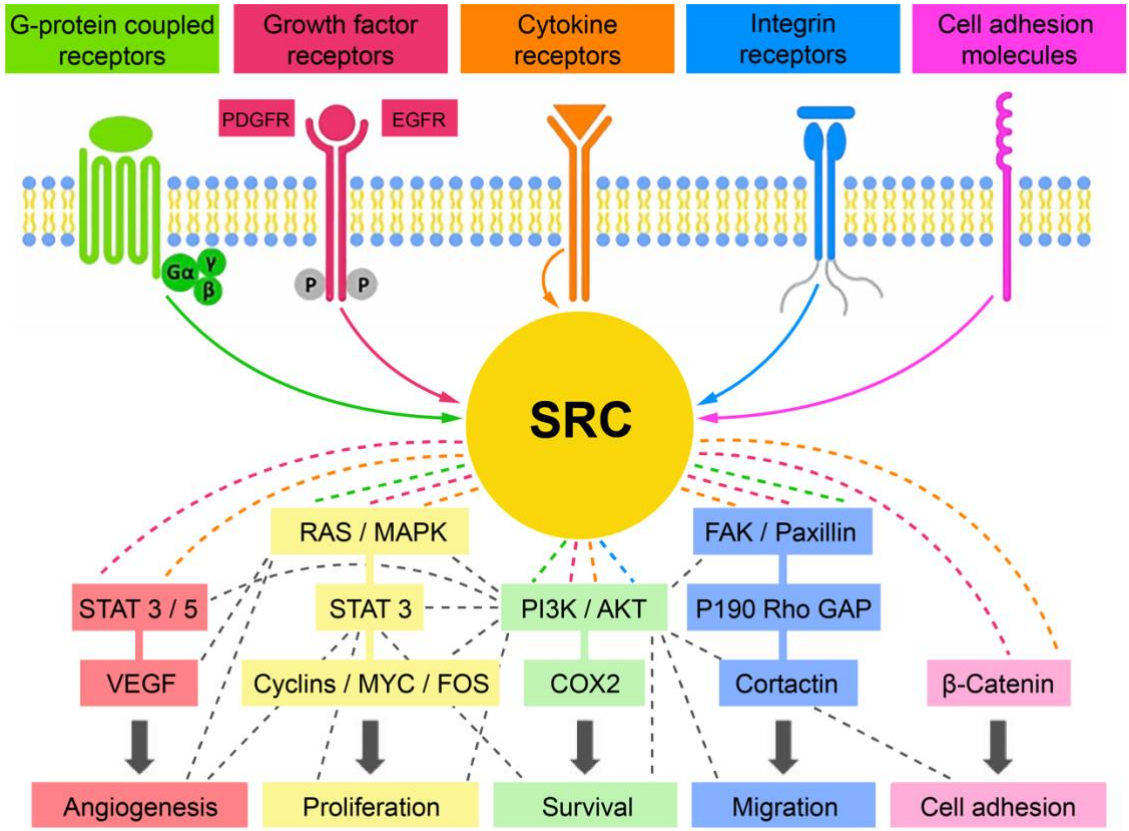

Figure 10. Simplified examples of SRC-mediated signal transduction pathways. Extracellular ligands bind to transmembrane protein receptors. When activated, SRC phosphorylates diverse targets transducing these signals into cellular pathways of angiogenesis, proliferation, survival, migration and cell adhesion.

Many tumors (especially breast, colorectal, prostate, pancreatic and gastric carcinoma) are associated with amplifications and / or overexpression of SRC, and are also related to elevated levels of growth factors and SRC's downstream proteins such as focal adhesion kinase (FAK) and signal transducer and activator of transcription 3 (STAT 3).[59] In hepatocellular carcinoma, increased SRC activity has been observed as a result of reduced levels of inhibitory CSK.[60] By contrast, colorectal cancer is associated with activating mutations.[61] However, elevated *SRC* expression is unlikely to directly condition cancer cell growth.[59] Instead, up-regulation of downstream proteins allows for growth factor independency and stepwise facilitates tumor progression from immortalization of malignant cells to invasion and metastases.[62]

In order to provide a better understanding of SRC's role in cancer, exemplary SRC-mediated signaling pathways and their impact on carcinogenesis are discussed in the following.

One of Src kinase's major functions is the control of cytoskeleton arrangement. This is achieved by close cooperation with growth factors (for example EGF) and integrins in contact with p190 Rho GTPase activating protein (antagonizes Rho-dependent contractility), cortactin and focal adhesion proteins like FAK or paxillin.[62] The relation of SRC and EGF was clarified in breast cancer showing abundant activity of both factors with SRC potentiating the mitogenic responsiveness to EGF stimulation.[63]

FAK, one of SRC's key binding partners bundles integrin- and growth factor-induced signals required for cell dispersion, morphological change and accelerated division.[64] In case of disrupted signaling, it seems to enhance tumor cell sensitivity for misguided migration and epithelial-mesenchymal transition.[65]

Cell integrity is further maintained by SRC's regulation of the β-Catenin / E-Cadherin complex. Phosphorylation of this cell-cell adhesion complex by constitutively active Src kinase results in an impairment of cell differentiation, dissemination and invasiveness.[66]

Moreover, SRC stimulates STAT- and VEGF- driven angiogenesis and vascular permeability.[67]

By regulating the PI3K / AKT pathway, SRC influences a diversity of cellular events like cell adhesion and migration, differentiation, DNA synthesis and most of all survival which is also an objective of Cyclooxygenase 2 (COX2) stimulation.[56]

SRC activating the RAS / MAPK pathway with subsequently induced transcription factors for cell growth, division and apoptosis like STAT 3, MYC or FOS and their control of cyclins and cyclin dependent kinases represents a major proliferation stimulus.[55,62]

All in all, SRC's interactive properties enlarge the signals of affiliated pathways creating synergistic effects.[56]

Inhibiting Src kinase therefore seems to be a therapeutic rationale. Dasatinib (BMS-354825) and Bosutinib (SKI-6606), the two best studied SRC (and BCR-ABL) tyrosine kinase inhibitors, are FDA approved for hematologic malignancies and are currently tested in solid cancers like breast, colon and prostate carcinoma.[59] Human cell lines derived from these solid cancer types not only showed suppressed proliferation, but also a decline in dysfunctional adhesion, migration and invasiveness after being exposed to Dasatinib.[68,69] SRC inhibitors prevented primary tumor growth and metastatic spread in mice with prostate carcinoma xenografts *in vivo*.[70] In a pancreatic adenocarcinoma mouse model, Dasatinib inhibited metastases and reduced the primary tumor size, which emphasizes its better success in cutting dissemination than in suppressing tumor emergence.[62,71] Regarding SI-NETs, SRC inhibition *in vitro* and *in vivo* arrests tumor growth.[72]

Due to its clinical effectiveness and tolerability in phase 1 and phase 2 trials with adverse effects comparable to other therapies (fatigue, neutropenia, pleural effusion), Dasatinib is soon expected to be FDA approved for solid tumors.[73]

On one hand, cytostatic SRC blockade is worrisome because of the wide range of affected downstream proteins, of which many are required for essential cell activities. On the other hand, synergistic anti-cancer effects have been noticed resulting from mutual inhibition of SRC and its closely related signaling partners. As an example, silenced SRC increased the sensitivity to Cetuximab (EGFR inhibitory monoclonal antibody) in colorectal carcinoma and non-small cell lung cancer in preclinical studies.[74,75] Since many of Src's activators are receptor tyrosine kinases, multikinase inhibition could amplify the effect of blocking SRC's excessive activity.

1.5. Aim of the thesis

Neuroendocrine tumors of the small intestine are rare but represent the most frequent small bowel malignancy. Their late manifestation associated with an extensive metastatic spread has a limiting impact on surgery as the only curative treatment. It is obvious that a better understanding of the molecular mechanisms

underlying these tumors is required for the development of promising targeted therapies.

AURKA as a key mitotic regulator gene and *SRC* as one of the first discovered proto-oncogenes have been identified as amplified and / or overexpressed in a variety of malignancies. This thesis, in particular, focuses on *AURKA* and *SRC* alterations in SI-NETs and on numeric aberrations of chromosome 20 which harbors both genes. Since the whole exome sequencing study by Banck *et al.* comprised a small cohort of only 48 patients, the analysis of *AURKA* and *SRC*'s roles in the emergence of SI-NETs is extended in this thesis.[28] For this purpose, 217 tissue samples of 135 patients, arranged as Tissue Microarrays (TMAs) were examined by fluorescence *in situ* hybridization (FISH). Protein expression levels of AURKA and SRC were determined *via* immunohistochemistry (IHC). Moreover, catalytic activity was examined with specific antibodies targeting phosphorylation site Thr_{288} for AURKA and Tyr_{527} for SRC.

Since the inhibition of protein kinases achieved therapeutic success in various cancer types, Aurora A inhibitors like Alisertib and Danusertib are currently tested in advanced clinical trials showing considerable effects *in vitro* and *in vivo*. Src tyrosine kinase inhibitors such as Bosutinib and Dasatinib are already FDA approved and in clinical use.

With regard to new potential approaches to SI-NET therapy, it is of great importance to verify the reported alterations using different methods.[28] An understanding of how these alterations affect tumor emergence and progression could provide additional information for optimizing the therapeutical schedule.

2. Material and methods

2.1. Patients and samples

For this investigation, 217 SI-NET samples were gained by surgical resection including 128 primary tumors (from the jejunum, ileum and the iliocaecal valve), 74 lymph node metastases and 15 distant (mostly hepatic) metastases from 135 patients. In many cases, patients provided a primary tumor and its corresponding node and / or distant metastasis.

The study obtained ethical approval from the local ethics committee at the University Hospital of Tuebingen (469 / 2010BO2).

After formalin fixation, paraffin embedding and hematoxylin and eosin (H&E) staining, the samples were evaluated as well-differentiated tumor tissue according to the WHO classification by a pathologist *via* light microscopy at the pathology departments of Tuebingen, Munich, Duesseldorf or Marburg. Then the tissue was staged according to the UICC TNM criteria and additionally classified by an internal score with the first group (encoded 1) listing all UICC stages separately, the second group (encoded 2) combining UICC stages I to IIB (other stages separately) and the third group (encoded 3) combining UICC stages I to IIIA (other stages separately).

Depending on tumor spread at the time of diagnosis the patients were grouped into three cohorts; (1) patients with only primary tumors, (2) patients with additionally lymph node metastases and (3) patients with both node and distant metastases.

2.2. Tissue microarray

Formalin-fixed paraffin-embedded (FFPE) tissues (see 2.1. Patients and samples) were used to fabricate eight tissue microarrays (TMA) by Christine Beschorner and Dr. Maike Nieser (working group of Prof. Sipos). Tissue samples with a size of 1 mm were taken from donor paraffin blocks and placed into pre-punched gaps of recipient paraffin blocks in duplicate (TMA 6, 7, 8) and in

triplicate (TMA 11.1, 11.2, 12, 13, 14) using a tissue microarrayer (Beecher Instruments, WI, USA) and MTABooster (Alphelys, Plaisir, France). TMA grid layouts were created with the TMA Designer 2 software (Alphelys, Plaisir, France). The recipient paraffin blocks were first treated at 56 °C for 10 minutes and subsequently at 4 °C for 30 minutes. This sealing procedure was repeated twice. For both immunohistochemistry and fluorescence *in situ* hybridization, thin sections of 3 or 3.5 µm were separated from the TMA blocks and applied on SuperFrost Plus slides (Langenbrinck, Emmendingen, DE).

2.3. Chemicals and equipment

Table 4. Chemicals

Chemicals	**Manufacturer**
Double-distilled water (ddH_2O)	Merck (Darmstadt, Germany)
Ethanol 100%	Merck (Darmstadt, Germany)
Hydrogen peroxide 30%	Merck (Darmstadt, Germany)
Pepsin	Sigma-Aldrich (St. Louis, MO, USA)
ProLong® Gold Antifade mountant with DAPI	Thermo Fisher Scientific (Waltham, MA, USA)
Sodium chloride	Merck (Darmstadt, Germany)
Sodium citrate	Sigma-Aldrich (St. Louis, MO, USA)
Xylene AnalaR NORMAPUR ACS	VWR Chemicals (Radnor, PA, USA)
Zytochem-Plus HRP Polymer-Kit	Zytomed Systems (Berlin, Germany)

Table 5. Buffers

Buffers	Manufacturer / Composition
Ammonia solution 25%	Merck (Darmstadt, Germany)
Papanicolaou's solution 1a Harris' hematoxylin solution	Merck (Darmstadt, Germany)
Wash buffer (20x)	Zytomed Systems (Berlin, Germany)
Citrate buffer (10x, pH 6)	29.4 g Trisodium citrate dihydrate ad 1 l ddH_2O
Post-hybridization wash buffer (0.3% NP-40 / 2x SSC)	100 ml 20x SSC (pH 5.3) 3 ml NP-40 ad 1 l ddH_2O
Saline sodium citrate (SSC) buffer (20x, pH 7.4)	175.32 g Sodium chloride 88.23 g Sodium citrate ad 1 l ddH_2O
TEC buffer (10x, pH 9)	2.5 g Tris(hydroxymethyl)aminomethane 5 g Ethylene diamine tetraacetic acid 3.2 g Trisodium citrate dihydrate ad 1 l ddH_2O

Table 6. Consumable supplies

Consumable supplies	Manufacturer
Cover slips	Menzel (Braunschweig, Germany)
Glass slides	R. Langenbrinck (Emmendingen, Germany)
Pipettes (10 µl, 100 µl, 200 µl, 1000 µl)	Eppendorf (Hamburg, Germany)
Pipette tips	Starlab (Blakelands, UK)
Reaction tubes 1.5 / 2 ml	Eppendorf (Hamburg, Germany)
SuperFrost Plus slides	R. Langenbrinck (Emmendingen, Germany)

Table 7. Equipment

Equipment	Manufacturer
AxioCam MRm	Carl Zeiss MicroImaging (Goettingen, Germany)
Centrifuge	Eppendorf (Hamburg, Germany)
Fluorescence microscope Axio Imager M2	Carl Zeiss MicroImaging (Goettingen, Germany)
Microscope	Carl Zeiss (Jena, Germany)
MiraxDesk Scanner	Carl Zeiss (Jena, Germany)
ThermoBrite Stat Spin	Abbott Molecular (Abbott Park, IL, USA)
Thermomixer Comfort	Eppendorf (Hamburg, Germany)
Tissue Microarrayer	Beecher Instruments (Sun Prairie, WI, USA)
Ventana BenchMark System	Ventana Medical Systems (Tucson, AZ, USA)
Vortex mixer	IKA (Staufen im Breisgau, Germany)
Water bath	GFL Gesellschaft für Labortechnik (Burgwedel, Germany)

Table 8. Antibodies / Probes

Antibodies / Probes	**Manufacturer**
AURKA (polyclonal antibody produced in rabbit) #HPA002636	Sigma-Aldrich (St. Louis, MO, USA)
p-AURKA (pT288, polyclonal antibody produced in rabbit) #PAB25906	Abnova (Taipei City, Taiwan)
p-SRC (Y527, polyclonal antibody produced in rabbit) #2105S	Cell Signaling Technology (Danvers, Massachusetts, USA)
SRC (36D10, monoclonal antibody produced in rabbit) #2109	Cell Signaling Technology (Danvers, Massachusetts, USA)
AURKA / CEN20p FISH probe #FG0132 (Texas Red / FITC)	Abnova (Taipei City, Taiwan)
CEN20q FISH probe #FC0166 (FITC)	Abnova (Taipei City, Taiwan)
SRC / CEN20p FISH probe #FG0175 (Texas Red / FITC)	Abnova (Taipei City, Taiwan)

Table 9. Software

Software	**Manufacturer**
MTABooster	Alphelys (Plaisir, France)
Tissue Studio XD 2.3.0	Definiens (Munich, Germany)
TMA Designer 2	Alphelys (Plaisir, France)
SPSS Statistics 24	IBM (Armonk, NY, USA)

2.4. Fluorescence in situ hybridization

Fluorescence *in situ* hybridization (FISH) is a diagnostic and clinical research technique based on the binding of labeled DNA or RNA sequences to target genes or chromosome segments in interphase or metaphase cells allowing for the investigation of genetic aberrations. In particular, short locus-specific complementary single-stranded DNA sequences (probes) are used to detect the

location, gain or loss of genes and structural or numerical chromosomal abnormalities. In cancer diagnosis and therapy, FISH can determine the etiopathogenesis and the progression level of a disease.[76]

For the preparation process the probes have to be isolated from fragmented DNA gained from plasmids, cosmids, several artificial chromosomes like yeast artificial chromosomes (YACs) and other sources.[77] When processed and amplified, a fluorescent dye is added to the probes in order to localize the hybridization. Therefore, the probes are labeled by chemical or enzymatic reactions such as nick translation or polymerase chain reaction (PCR) and are either directly marked by fluorophores or indirectly by attaching them to a hapten reporter molecule such as biotin, dioxigenin, aminoacetylfluorene, dinitrophenyl or sulfonate tagged with an antibody binding a corresponding fluorescence marked anti-immunoglobulin.[78] The most typical fluorescent dyes are Texas Red, fluorescein isothiocyanate (FITC) and rhodamine. Figure 11 illustrates the hybridization of the target DNA and the labeled probe.

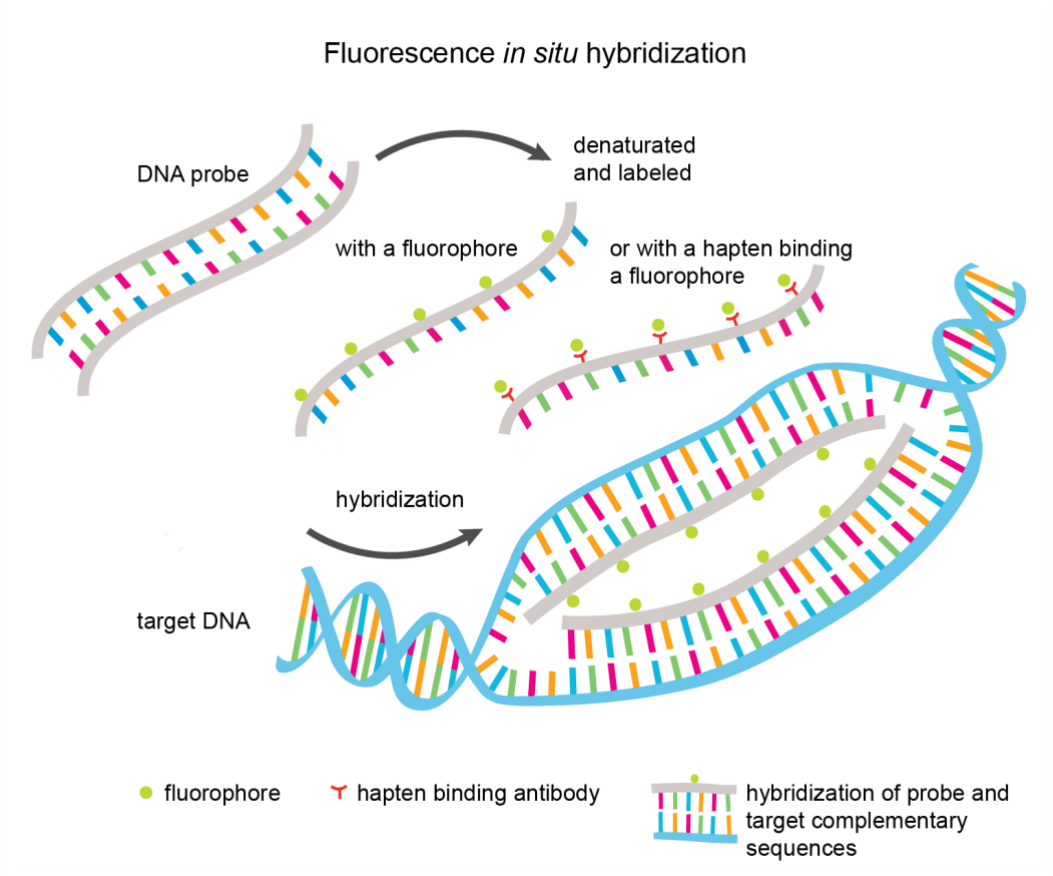

Figure 11. Fluorescence *in situ* hybridization technique. The probe is either marked with a fluorophore or with a fluorophore bound to a hapten, signaling the existence / quantity of the target. Modified according to: http://www.abnova.com/images/content/support/FISH_brochures.pdf. Date accessed: 06/04/2017.

This method can be used for the analysis of both paraffin-embedded and frozen tissue.

In this study, FISH was performed following the protocol given below. In order to examine *SRC* and *AURKA* and compare the count of chromosome 20 in formalin-fixed and paraffin-embedded TMAs, Abnova AURKA/CEN20p FISH probe #FG0132 and Abnova SRC/CEN20p FISH probe #FG0175 (Taipei City, Taiwan) were used, both of which are mixtures with one probe targeting the gene of interest and the other one the corresponding chromosomal centromere. Additionally, chromosome 20 was tested with the Abnova CEN20q centromere FISH probe #FC0166.

Protocol for FISH (Abnova). During paraffin-embedded tissue pretreatment, the samples first were deparaffinized in xylene three times for five minutes each at room temperature. Then they were immersed in 100% ethanol twice for five minutes each at room temperature and air-dried. Afterwards, the slides were treated with a sodium citrate paraffin pretreatment solution at 95°C for 30 minutes and subsequently washed with a saline sodium citrate wash buffer (2 x SSC) for five minutes twice. To improve the DNA accessibility and reduce background such as cytosolic auto fluorescence the samples were treated with a pepsin solution as digestive protease treatment at 37°C for six minutes and subsequently washed (see above). Regarding tissue integrity, excessive protease treatment generally should be avoided. The last step of the pretreatment consisted of tissue dehydration in 70% ethanol and then in 100% ethanol for one minute each at room temperature and air-drying.

After applying the FISH probe (in this case 10 µl for a 22 x 22 mm tissue area) the slides were covered with cover glass, sealed with rubber cement and denatured at 75°C for 5 minutes.

The denatured target DNA was incubated with the probe in a humidified box at 37°C for 48 hours, which allowed for the hybridization of their single strands through the formation of hydrogen bonds.

Post-hybridization washing was used to remove residual DNA and probe. For this purpose, rubber cement and cover glass were removed, the samples were washed with 2 x SSC wash buffer for five minutes at room temperature, then with post-hybridization wash buffer 2 x SSC / 0,3% NP-40 at 73°C for two minutes and lastly with 2 x SSC wash buffer for one minute at room temperature.

Eventually, the target area was counterstained with 10 µl DAPI (4’6’-Diamidine-2’-phenylindole dihydrochloride), cover slipped and sealed with manicure.

FISH evaluation. To evaluate the FISH, signals were examined in at least 30 cells per sample *via* fluorescence microscopy with a Zeiss Axio Imager M2 microscope (Oberkochen, Germany) equipped with a double filter for the simultaneous view of gene signals for *AURKA* or *SRC* (Texas Red) as well as the signal for chromosome 20 (FITC). Assuming there are two alleles of each

gene in a normal cell, 60 signals in 30 examined cells were considered as normal gene / chromosomal status. More signals (threshold was set at >72 target gene signal counts) could be ascribed to specific gene amplification or to polysomy, i.e. the presence of one or more additional chromosomes. Due to this differentiation, statistical analysis required a numeric relation of the target gene and the respective chromosome signal. Since chromosome 20 signals could not be consistently evaluated, setting up this ratio was not possible. Instead, the ratios of *AURKA* signals to *SRC* signals and vice versa were calculated with the denominator giving an estimation of the centromere signal. In this way, specific gene amplification was defined as ≤ 72 estimated centromere signal counts with a target to estimated centromere signal ratio > 1.2. In contrast, centromere signals > 72 with a ratio ≤ 1.2 were specified as polysomy. In case of simultaneous gene amplification and polysomy, centromere signal counts were > 72 with a ratio > 1.2.

2.5. Immunohistochemistry

Immunohistochemistry (IHC) is a tissue staining method combining immunology, histology and chemistry by using antibody-linked dyes to highlight antigens, i.e. specific structures within a tissue. There are different principles of immunostaining. Antibodies binding to epitopes are either directly marked or their Fc fragment is bound to a labeled secondary antibody. More precisely, the antibody is covalently bound to a catalytic enzyme, such as peroxidase or alkaline phosphatase. Once the antibody binds to the respective epitope the featured enzyme catalyzes a chromogenic substrate reaction with the oxidation of the chromogen (for example 3,3' Diaminobenzidine or 3-Amino-9-Ethylcarbazole) resulting in a color signal. The signal can be amplified by tagging the antibody with a biotin-avidin complex, a biotin-streptavidin complex or with a polymer-based detection system. Antibodies are mostly produced in rabbits or mice and can be both monoclonal (high specificity for a single epitope) and polyclonal (lower specificity and higher likelihood of cross-reaction with similar epitopes).[79] Figure 12 illustrates the different immunohistochemical staining methods.

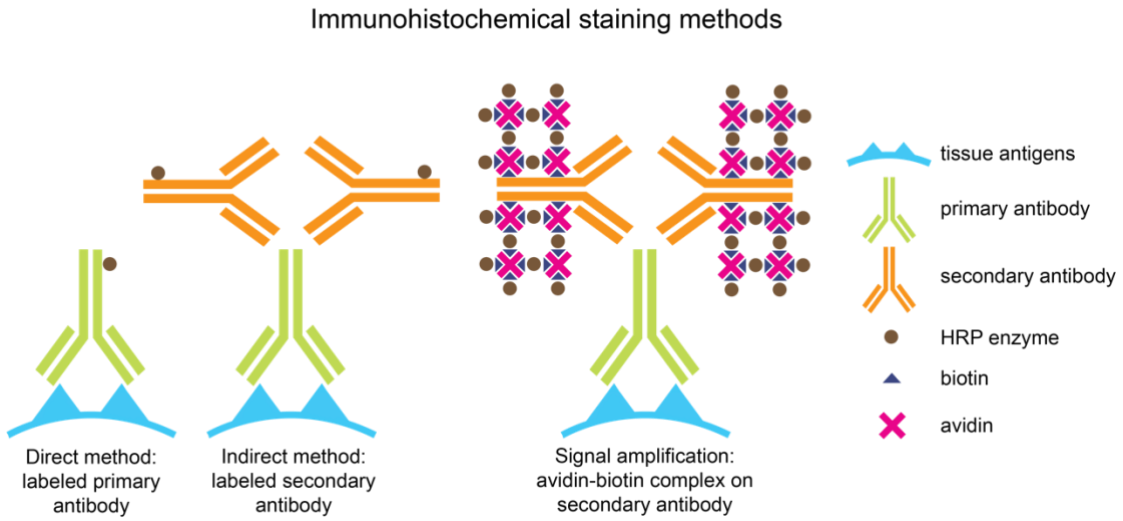

Figure 12. Immunohistochemical staining methods. Direct method, indirect method and signal amplification. Modified according to: http://www.immunohistochemistry.us/immunohistochemistry-staining.html and https://www.novusbio.com/ihc-detection. Date accessed: 06/04/2017.

As a standard diagnostic method, immunohistochemistry is used to trace the origin of tumors and infectious diseases.[80] There are specific immunohistochemical markers for various neoplasms. Specific clusters of differentiation are for example indicative of hematopoietic and lymphoid malignancies, whereas cytokeratins mark epithelial tumors.[81] In addition, immunohistochemistry can determine apoptosis, mitosis or proliferation with particular markers of which Ki-&7 is a well-known representative.[82,83] As a result, it improves the assessment of a disease's characteristics so that it can be classified, given a prognostic value and a predicted treatment response.[84]

The method can be applied to frozen tissue and formalin-fixed paraffin-embedded tissue.

In this study, the samples were examined for AURKA (nuclear and cytoplasmic) and SRC (cytoplasmic) expression. Phospho-AURKA und phospho-SRC were also tested but did not show remarkable results. For this purpose, tissue was immunostained with Sigma-Aldrich AURKA Cat#HPA002636 (St. Louis, USA), Abnova phospho-AURKA (pT288) Cat#PAB25906 (Taipei City, Taiwan), both polyclonal antibodies produced in rabbits, Cell Signaling SRC (36D10,

monoclonal antibody produced in rabbits) Cat#2109 and Cell Signaling phospho-SRC (Y527, polyclonal antibody produced in rabbits) Cat#2105S (Cambridge, UK) at the Institute of Pathology, University of Tuebingen. The AURKA antibody was established on a colon carcinoma TMA which was also used as positive control due to its close resemblance to tissue of the small intestine. For the SRC antibody tonsil tissue was used as positive control because of strong cytoplasmic SRC expression in lymphoid tissue. The antibody was also established on a tonsil block. The slides were stained both manually and with an autostainer (Ventana BenchMark System,Tucson, USA) for checking purposes.

Protocol for IHC. Starting with a paraffin-embedded tissue pretreatment, the samples were deparaffinized in xylene three times for 15 minutes each at room temperature. For rehydration, they were immersed for three minutes in 100% ethanol twice, for three minutes in 96% ethanol twice and for three minutes in 75% ethanol. To inactivate the endogenous peroxidase, the slides were incubated with 3% hydrogen peroxide in 75% ethanol for five minutes. Afterwards, the slides were rinsed in distilled water for five minutes.

The epitopes were retrieved with a heat-based treatment reversing the cross-links formed during fixation. For this purpose, the samples were boiled in sodium citrate (pH 6, for AURKA) and TEC (pH 9, for SRC) buffer for five minutes. After cooling down for 20 minutes, the slides were briefly immersed in distilled water and rinsed in wash buffer for three minutes twice.

For hybridization, antibodies were applied overnight. The next day, the slides were rinsed in wash buffer for five minutes, followed by the application of the secondary antibody (PostBlock) for 30 minutes, re-washing (see above) and the application of the horseradish peroxidase polymer (HRP) conjugate for another 30 minutes. After re-washing (see above) the tissue was covered with 3,3’ Diaminobenzidine (DAB) for five minutes twice. The oxidation of DAB catalyzed by HRP caused a brown staining.

Subsequently, the samples were re-washed, briefly immersed in distilled water and then counterstained with Papanicolaou’s solution for 15 seconds enhancing cell identification. Afterwards, the slides were briefly rinsed in distilled water three

times, then immersed in an ammonia solution (6 ml 3% ammonia in 200 ml 70% ethanol), followed by dehydration in 70% ethanol for two minutes, 80% ethanol for two minutes, 96% ethanol for two minutes twice, 100% ethanol for two minutes four times and xylene for two minutes four times. Eventually, a cover slip was applied.

IHC evaluation. The immunostainings were analyzed using light microscopy (Carl Zeiss, Oberkochen, Germany). For AURKA the staining intensity ranged from 0 to 3 (0: negative, 1: weakly, 2: moderately, 3: strongly positive) for both nuclear and cytoplasmic signals. For SRC, the immunoreactive score (IRS) was used taking account of the cytoplasmic staining intensity (0: negative, 1: weakly, 2: moderately, 3: strongly positive) multiplied with the quantity of positive cells (0: none, 1: <10%, 2: 10-50%, 3: 51-80%, 4: >80%). The results ranging from 0 to 12 were evaluated according to the Remmele score (0-2: negative, 3-4: weakly, 6-8: moderately, 9-12: strongly positive) and *via* dichotomic division (0-6: negative – moderate and 7-12: strong).

Additionally, the AURKA slides were scanned (MiraxDesk Scanner, Carl Zeiss, Jena, Germany) and evaluated with Tissue Studio XD 2.3.0 (Definiens, Munich, Germany). This software provided quantitative tissue analysis by scaling the staining extent and intensity of nuclear antigens in relation to the total area of selected regions of interest. The thresholds of weak to moderate and moderate to high hematoxylin and IHC staining intensity were set with the nucleus classification tool. As a result, the percentage of moderately and strongly AURKA expressing cells compared with all investigated cells was calculated as a quantitative reference for the manual evaluation. Figure 13 visualizes the Definiens Tissue Studio workflow starting with an appropriate grid view selection (a) proceeding to the nucleus detection (b) and intensity classification (c), which enabled the final calculation.

Since this software only provides reasonable results for nuclear protein expression it could not be applied to SRC evaluation.

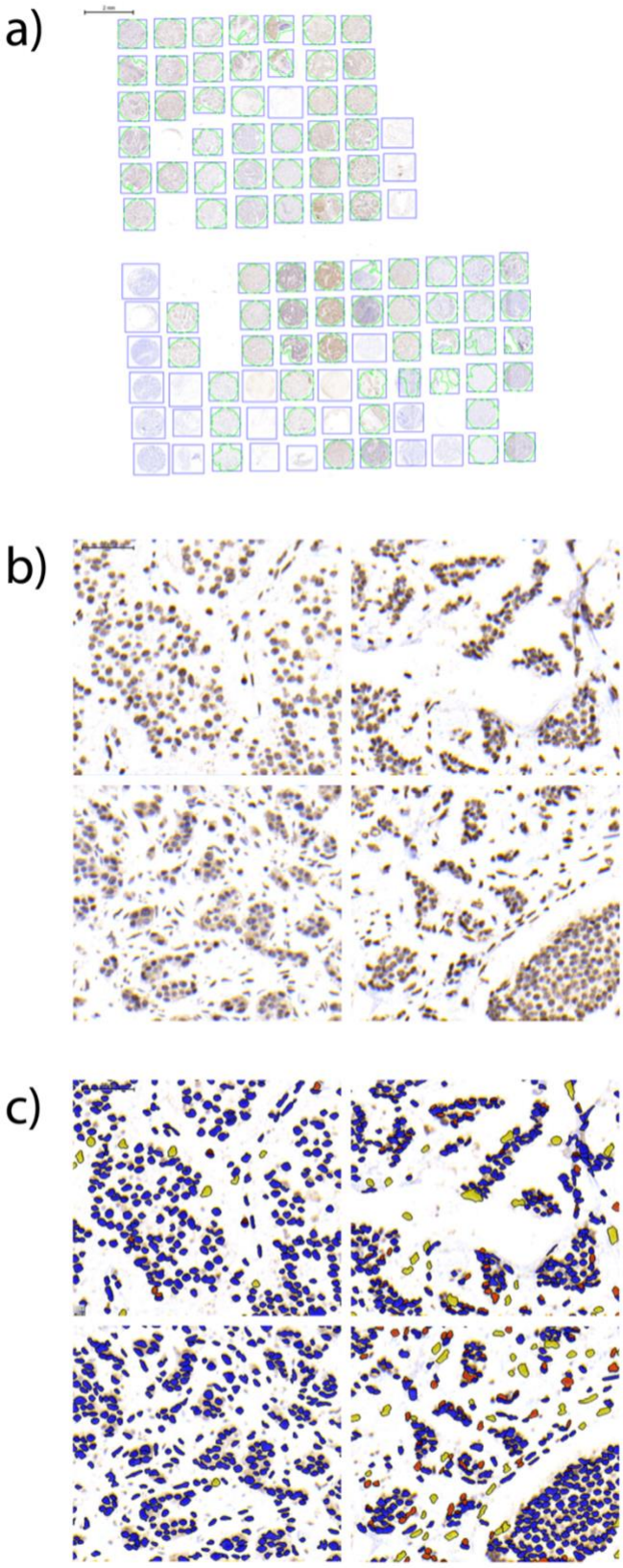

Figure 13. Definiens Tissue Studio 2.3.0. workflow. a) Qualified samples are chosen with a grid view selection, b) nucleus detection determines nuclear morphologies, c) staining intensity thresholds are set by nucleus classification.

2.6. Statistical analysis

The findings for AURKA and SRC provided by FISH and IHC were statistically tested for correlations between amplification and overexpression depending on the spreading progress of the tumors. Thereby, the results for (1) primary tumors, (2) lymph node metastases, (3) distant metastases and (4) any clinical case (irrespective of the origins mentioned before) were separately examined.

As part of this analysis, FISH copy numbers were compared to IHC results *via* Pearson's chi-square test in two different settings. First, the IHC results were split up by the immunoreactive score (IRS) into negative and weakly stained (IRS 0-3) on one hand and moderately and strongly stained (IRS 4-12) on the other. Second, the results were organized dichotomously (IRS 0-6 and 7-12).

Similarly, Pearson's chi-square test was applied for the analysis of associations with other clinical characteristics.

The relation of FISH results and overall survival was analyzed with the Kaplan-Meier estimator.

Statistic dependencies were evaluated with SPSS (Statistics 24, IBM, Armonk, USA) with probabilities of $p < 0.05$ considered statistically significant.

3. Results

3.1. Patient and tumor specifications

In consideration of available data, 52% of the tissue donating SI-NET patients were male, 48% were female. The average age was 59 years with a standard deviation of 13 years, ranging from 20 to 87 years. Overall survival reached 31% with a median of 53 months. The tumor size ranged from 0.2 to 6.0 cm in diameter and was 1.9 cm on average.

Due to tissue insufficiency, 27 TMA samples could not be evaluated. As a result, 190 of 217 samples were validated, with 108 applicable cases for primary tumors, 68 for lymph node metastases and 14 for distant metastases. Since many patients provided matching pairs of primary tumor and metastasis, 115 clinical cases were validated without regard to primary or secondary (metastasic) provenance of the tissue.

Relating to the UICC TNM criteria, 6% of the samples (7/115) were assigned stage I, 5% (6/115) stage IIA, 4% (5/115) stage IIB, 0.9% (1/115) stage IIIA, 32% (37/115) stage IIIB, 48% (55/115) stage IV and in 3% (4/115) the stage was not identified. Stage IIIB and IV predominance corresponds with typically late clinical SI-NET manifestation.

The samples were tested for the expression of neuroendocrine biomarkers *via* IHC. 97% of the samples (174/180) featured synaptophysin (13% of which were weak, 40% moderate, 48% strong), 87% (156/180) were positive for serotonin (21% of which were weak, 18% moderate, 61% strong) and in 78% (140/180) SSTR expression was identified (19% weak of which were, 16% moderate, 65% strong).

3.2. AURKA signals determined by fluorescence in situ hybridization

3.2.1. *AURKA* signal count

Genetic alterations in SI-NETs were analyzed using FISH. A considerable part of 24% of the analyzed cases presented amplified *AURKA* signals, defined as >72

signals per 30 cells and detected as red spots (versus green centromere signals). In contrast to a normal signal count of 2, cells with *AURKA* amplifications displayed signals ranging from 3 to 6. The maximum signal number of the examined 30-cell units was 92. Figure 14 compares *AURKA* signals visualized by FISH in cells of an amplified case (a) to regular cells without amplifications (b) and provides a close-up view of cells of a second amplified case (c-f).

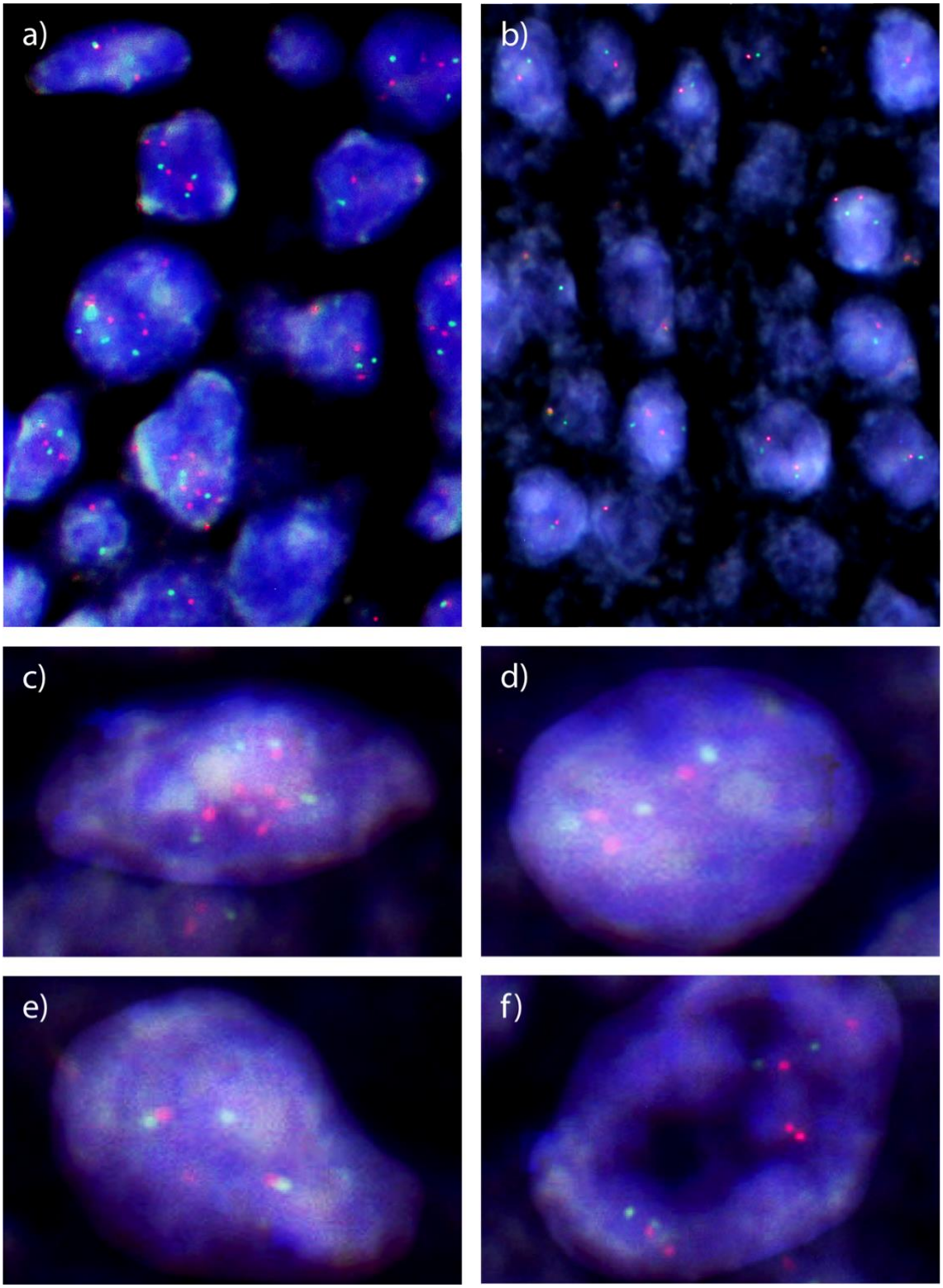

Figure 14. *AURKA* signals (red) visualized by FISH, magnification 1000x. a) An amplified case, b) a case without amplifications. c) – f) Close-up views of another amplified case display up to 6 signals per cell.

Amplifications were identified in 17% of the primary tumors, in 19% of the node metastases and in 14% of the distant metastases, calculated from 108 applicable cases for primary tumors, 68 for node metastases and 14 for distant metastases, as listed in Table 10. Figure 15 visualizes the distribution of amplifications subject to tumor progression.

Table 10. Percentage of *AURKA* copy number variations determined by FISH. P: primary tumor, LN: lymph node metastasis, DM: distant metastasis, Any: clinical cases irrespective of the spreading progress.

AURKA	**Applicable cases**	**Copy number variations**
P	108	17% (18/108)
LN	68	19% (13/68)
DM	14	14% (2/14)
Any	115	24% (27/115)

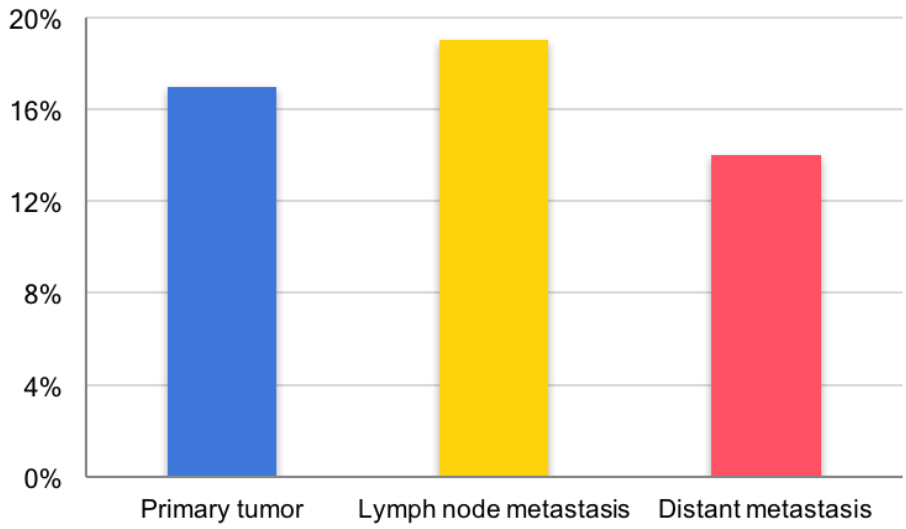

Figure 15. *AURKA* copy number variations grouped into primary tumor and metastases. Primary tumor, blue; lymph node metastasis, yellow; distant metastasis, red. Clinical cases n = 115.

An increased signal count can be based on different conditions: specific gene amplifications, polysomy or both at the same time, distinguishable by centromere signal and gene to centromere ratio (as described in 2.4.). The identified *AURKA* copy number gains were most frequently caused by polysomy (93%) with an

average centromere count of 77.3 (calculated from *SRC* signal counts due to inconsistent signal intensities of the centromere probe) and an average *AURKA* to centromere ratio of 1.02. However, a small amount (7%) of specific gene amplifications was detected.

3.2.2. Comparison of *AURKA* copy number gains to the findings of Banck *et al.*

The whole-exome study of Banck *et al.* included primary tumor sequencings of 48 patients. Thereby, *AURKA* amplifications were demonstrated in 25% (12/48) of the investigated cases.[28] Related to this analysis, a more detailed insight into the frequency and coherence of *AURKA* alterations was sought by the use of FISH. 135 clinical cases with 217 provided samples of primary tumor and metastases were taken into account for statistical computing, considerably exceeding the number of cases of Banck *et al.* This allowed for a more accurate statement about firstly, the representativeness of the overall results and secondly, the allocation of amplified cells in primary tumor and lymph node or distant metastases, which has not been discriminated by Banck *et al.* The comparison of copy number gains detected by FISH and WES (aligned by *AURKA*'s chromosomal position) yielded similar rates in both collectives.

3.2.3. Relationship between *AURKA* copy number gains and chromosome 18

Statistical analysis of *AURKA* copy numbers compared to loss of chromosome 18 as most frequent genetic alteration in SI-NETs identified a significant interdependency of increased *AURKA* signal counts and chromosome 18 loss in primary tumors ($p = 0.028$). The association of metastases and chromosome 18 was also tested but did not achieve a significant result.

3.2.4. Influence of *AURKA* copy number gains on tumor stage

Another question to consider is how *AURKA* signal enhancement interrelates with tumor stages. Copy numbers were statistically tested for correlation with TNM criteria and with an internal cluster of UICC stages (encoded 1, 2 and 3). TNM criteria did not seem to be affected by *AURKA* amplifications, neither in primary tumors, nor in metastases. While *AURKA* signal counts tested separately in primary tumor, lymph node and distant metastases did not correlate with tumor

progress, they showed a definite tendency when tested in all clinical cases. In particular, advanced tumors presented with significantly increased copy numbers (p = 0.049 for UICC stages IIIA-IV and 0.020 for stages IIIB-IV) than tumors of lower stages (taken into account as a collective, as discussed in 2.1.). The distribution of amplified cases by UICC tumor stage is outlined in Table 11. Figure 16 highlights the influence of *AURKA* amplifications on tumor progress in all clinical cases by comparing the rates of amplified to regular cases related to their corresponding UICC stage (clustered as encoded 3).

Table 11. *AURKA* copy number gains separated into UICC stages.

UICC stage	**Copy number gains**
I	0% (0/7)
IIA	0% (0/6)
IIB	20% (1/5)
IIIA	0% (0/1)
I - IIIA	5% (1/19)
IIIB	17% (6/36)
IV	34% (19/56)

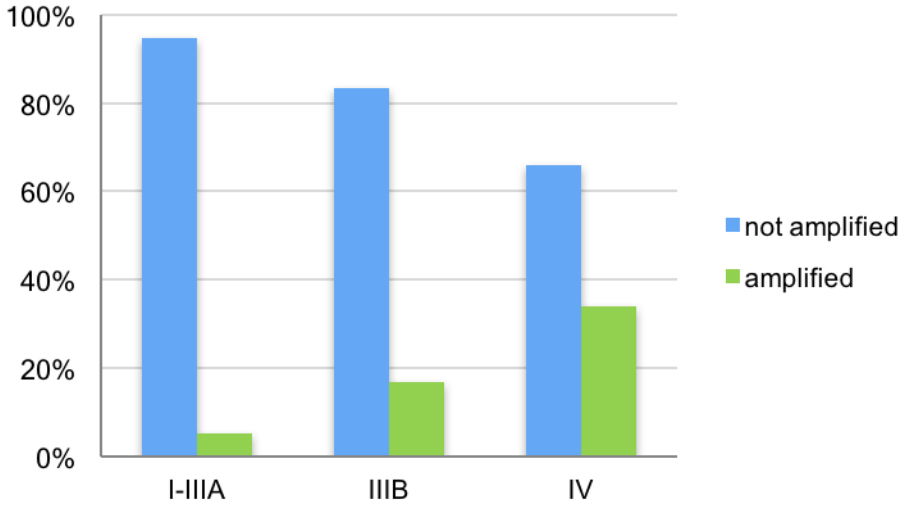

Figure 16. *AURKA* copy number gains matching UICC stage cluster. Clinical cases n = 111; p = 0.020. Not amplified, blue; amplified, green.

3.2.5. Correlation of *AURKA* copy number gains and survival

The impact of *AURKA* amplifications on overall survival was statistically tested with a Kaplan-Meier estimator for primary tumor and metastases both separately and combined. However, overall survival was not significantly affected by copy number gains. Figure 17 contrasts the Kaplan-Meier curves of amplified and regular cases taking into account all clinical cases without distinguishing primary tumor from metastases.

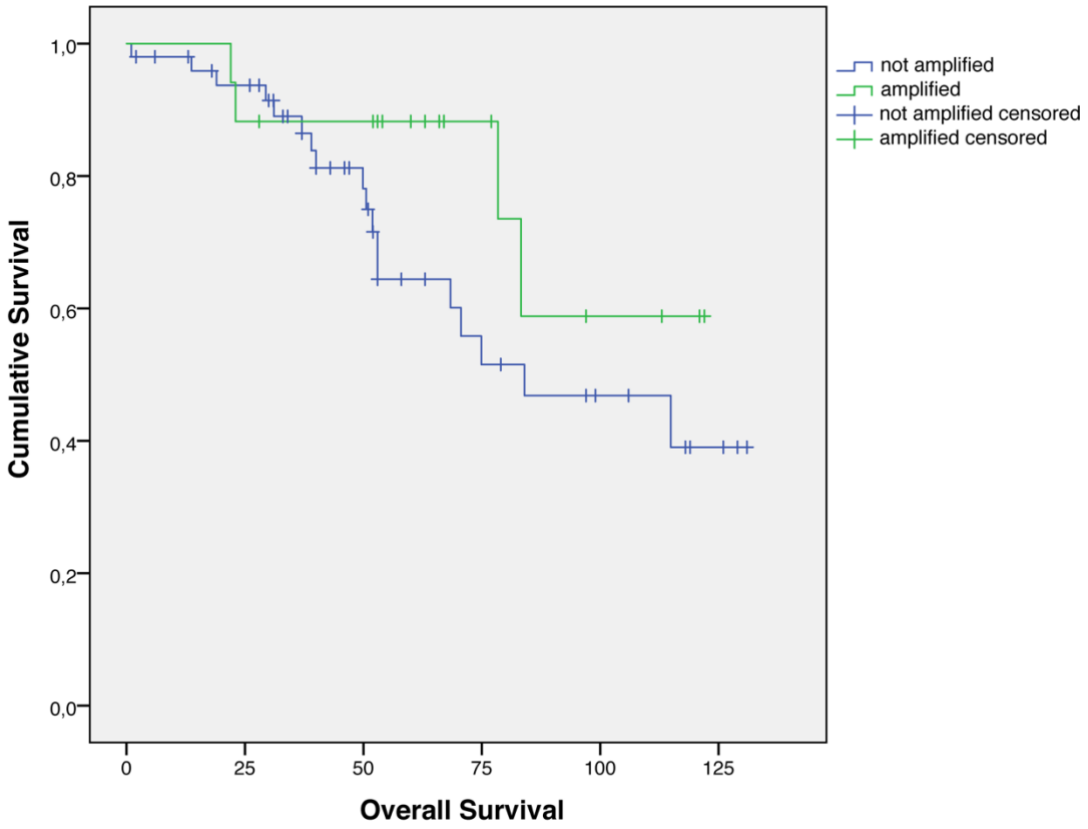

Figure 17. Kaplan-Meier survival curves of clinical cases with and without *AURKA* amplifications. Clinical cases n = 67; *p* = 0.191. Not amplified, blue; amplified, green.

3.3. AURKA protein expression analyzed by immunohistochemistry

3.3.1. AURKA protein expression intensity

The extent of AURKA expression was analyzed *via* IHC. Figure 18 shows an immunohistochemical staining of a representative SI-NET with high nuclear and moderate cytoplasmic AURKA expression. As indicated in Table 12, IHC verified moderate to strong nuclear expression in 56% of the primary tumors and 53% of the lymph node metastases. Distant metastases largely presented none or weak protein expression, with a minor part of moderate or high expression levels (21%). Cytoplasmic expression was mainly weak or not detectable. Moderate or strong protein expression was observed in 21% of the primary tumors, 12% of the lymph node metastases and 15% of the distant metastases.

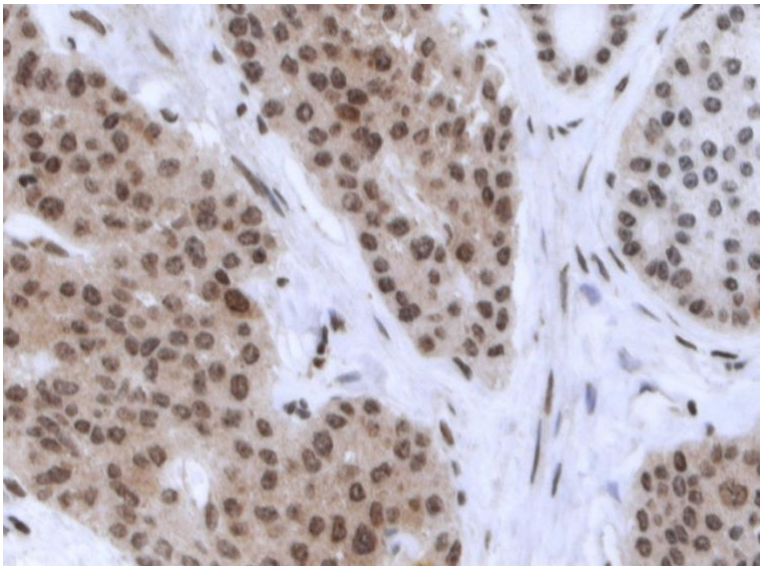

Figure 18. Immunohistochemical AURKA staining of a representative SI-NET tissue, magnification 400x. Moderate cytoplasmic expression (mid-brown), high nuclear expression (dark brown).

Table 12. Nuclear (nc) and cytoplasmic (cp) AURKA protein expression. Percentage of none / weak and moderate / strong stainings in primary tumors (P), lymph node metastases (LN), distant metastases (DM) and in all clinical cases irrespective of spreading progress (Any).

AURKA	Applicable cases	0-1 staining (none / weak)	2-3 staining (moderate / strong)
P (nc)	108	44% (48/108)	56% (60/108)
LN (nc)	68	47% (32/68)	53% (36/68)
DM (nc)	14	79% (11/14)	21% (3/14)
P (cp)	108	79% (85/108)	21% (23/108)
LN (cp)	68	88% (60/68)	12% (8/68)
DM (cp)	13	85% (11/13)	15% (2/13)
Any	115	22% (25/115)	78% (90/115)

Nuclear and cytoplasmic AURKA intensities are contrasted for primary tumors and metastases in Figure 19.

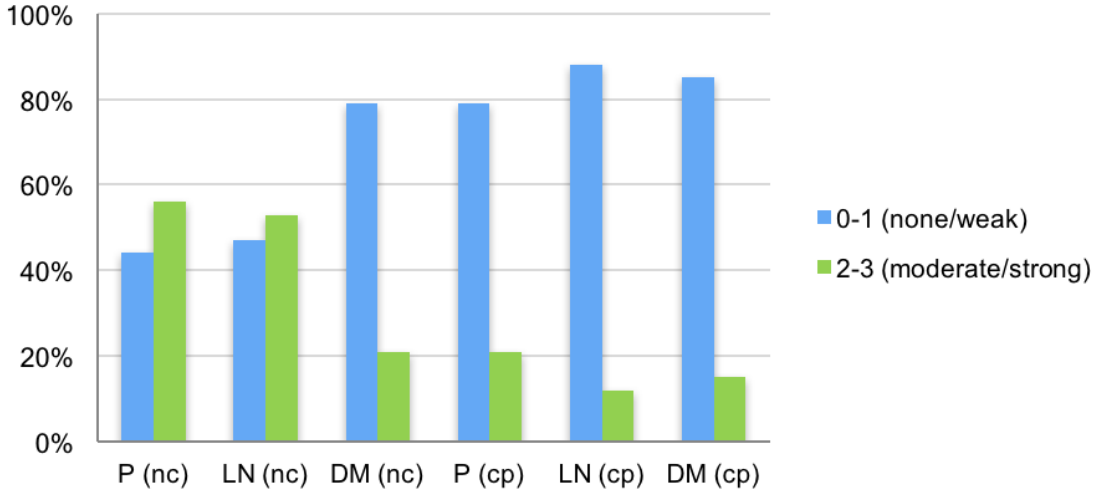

Figure 19. Nuclear (nc) and cytoplasmic (cp**)** AURKA protein expression in primary tumors (P), lymph node metastases (LN) and distant metastases (DM). None / weak expression, blue; moderate / strong expression, green.

3.3.2. Correlation of nuclear and cytoplasmic AURKA expression

The relationship between nuclear and cytoplasmic expression was statistically examined, including none, weak, moderate and strong stainings for primary tumors, lymph node metastases, distant metastases and all clinical cases (without regard to the spreading situation).

Nuclear protein expression was proved to significantly interrelate with cytoplasmic protein expression in all clinical cases (p = 0.042). In other words, patients exhibiting high nuclear Aurora A levels were likely to present high cytoplasmic protein levels as well. Taking account of primary tumors, lymph node and distant metastases separately, however, did not show significant correlation of nuclear and cytoplasmic protein expression. Eventually, another tendency became evident: primary tumors and lymph node metastases are most frequently characterized by weak cytoplasmic and moderate nuclear expression (28% of the primary tumors and 24% of the lymph node metastases) while the major part (31%) of distant metastases presented with low cytoplasmic expression but negative nuclei.

3.3.3. Effect of *AURKA* copy number gains on protein expression

In order to identify whether protein expression levels are related to increased *AURKA* signals, these variables were statistically analyzed. The test setting included matching pairs of FISH signals (amplified versus not amplified) on one hand and protein expression (non / weak vs. moderate / strong) on the other for primary tumors, lymph node metastases, distant metastases and all clinical cases combined. This analysis pointed out that there is no statistically significant influence of gene amplification on AURKA protein expression.

3.3.4. Correlation of AURKA expression and tumor progress

The association of Aurora kinase levels and tumor progress was tested in primary tumors and metastases in particular and in all clinical cases without regard to spreading. The testing correlated nuclear and cytoplasmic protein expression separately with TNM criteria and UICC stages. Considering UICC staging, significant results could not be detected. On the contrary, the test for TNM criteria disclosed a significantly high staining intensity in N stage tumors. This was verified for nuclear stainings of primary tumor samples ($p = 0.044$) and distant metastasis samples ($p = 0.005$) as well as for cytoplasmic stainings of distant metastases ($p = 0.007$). Correlations of protein expression and T or M stages, by contrast, could not be identified.

3.4. SRC signals determined by fluorescence in situ hybridization

3.4.1. *SRC* signal count

The analysis of *SRC* proto-oncogene in SI-NETs *via* FISH revealed amplified signals (defined as >72 signals per 30 cells, detected as red spots versus green centromere signals) in 25% of the clinical cases. In contrast to the regular signal count of 2, *SRC*-amplified cells reached 3 to 6 signals. The examined 30-cell units featured 95 signal counts at the maximum. Figure 20 demonstrates the difference between *SRC* signals in an amplified sample (a) and a case with regular copy numbers (b) and displays a close-up view of another sample with enhanced signals (c-f).

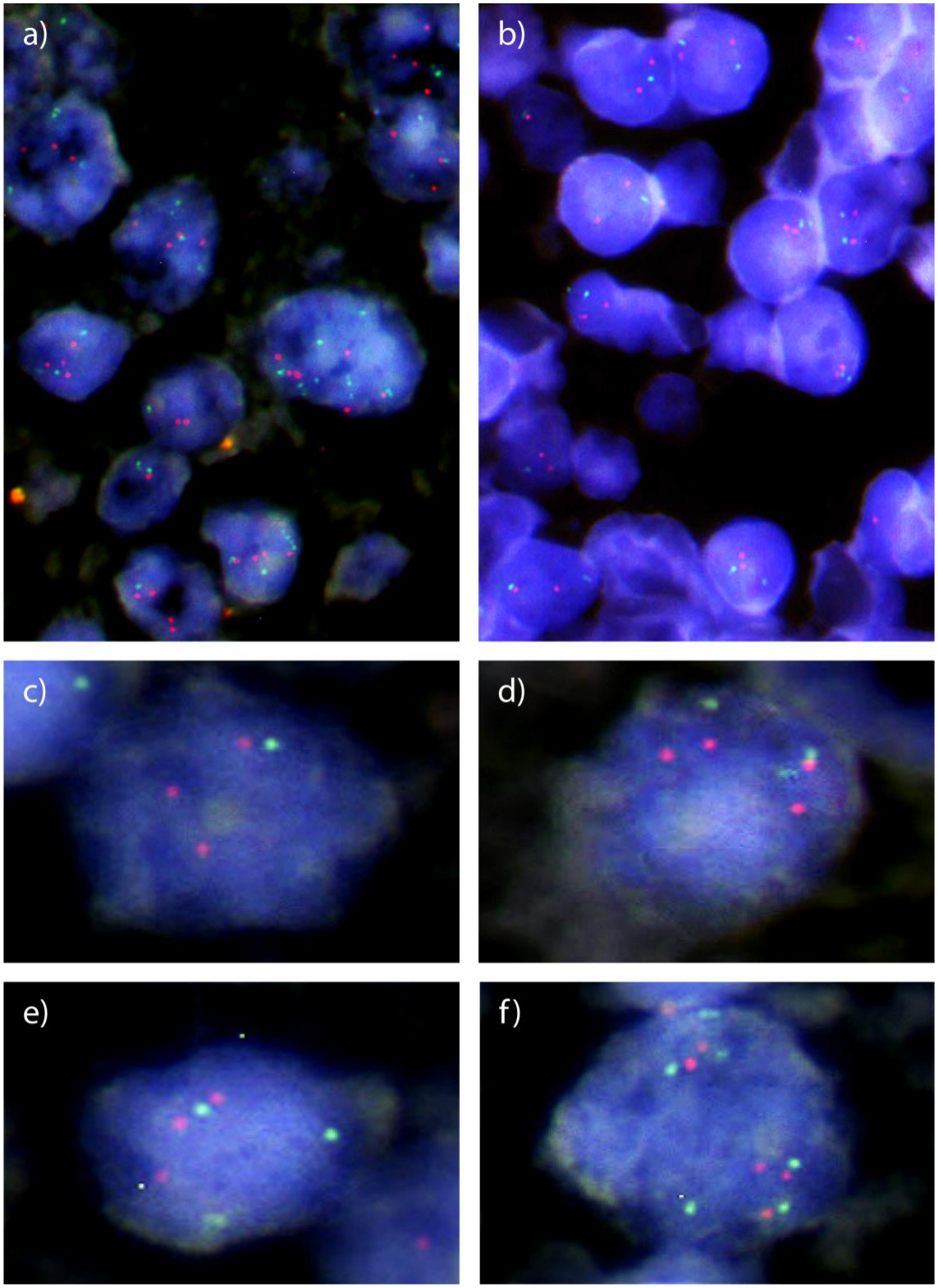

Figure 20. *SRC* signals (red) displayed by FISH, magnification 1000x. a) An amplified case, b) a case without amplifications. c) – f) Close up-views of another amplified case demonstrate up to 5 signals per cell.

Increased signal counts were identified in 18% of the primary tumors, but more frequently in lymph node metastases (28%) and in distant metastases (29%), as listed in Table 13 with regard to the valid cases of each fraction. The proportion of amplifications derived from primary tumors, lymph node and distant metastases is portrayed in Figure 21.

Table 13. *SRC* copy number variations determined by FISH. P: primary tumor, LN: lymph node metastasis, DM: distant metastasis, Any: clinical cases irrespective of spreading progress.

SRC	**Applicable cases**	**Copy number variations**
P	108	18% (19/108)
LN	68	28% (19/68)
DM	14	29% (4/14)
Any	115	25% (29/115)

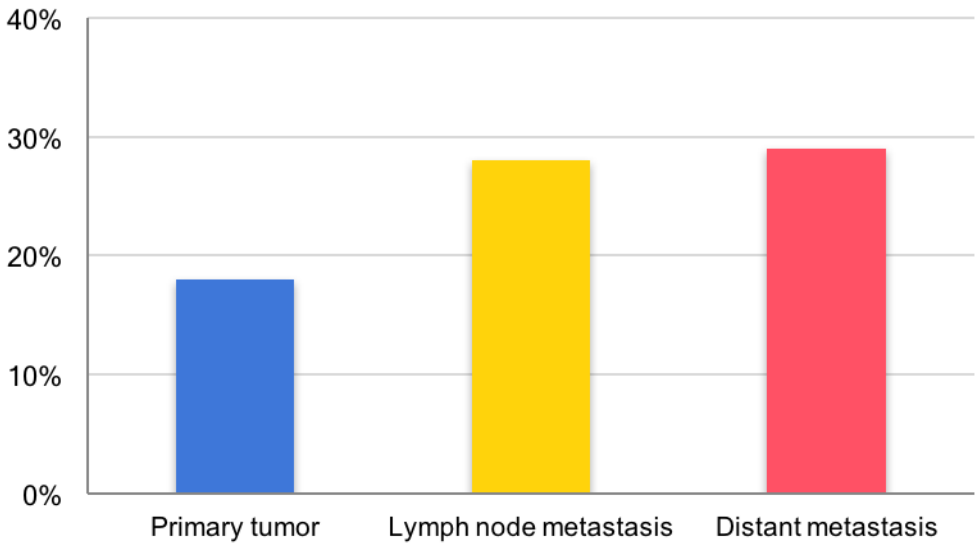

Figure 21. *SRC* copy number variations in primary tumors and metastases. Primary tumor, blue; lymph node metastasis, yellow; distant metastasis, red. Clinical cases n = 115.

Comparable to *AURKA*, *SRC* copy number gains largely (96%) resulted from polysomy of chromosome 20. The centromere mean count was 76.3 (calculated

from *AURKA* signals) with an average *SRC* to centromere ratio of 1.05. Only 4% of the increased signal counts could be derived from specific gene amplifications.

3.4.2. Comparison of *SRC* copy number gains to the findings of Banck *et al.*

In the sequencing study of Banck *et al. SRC* was amplified in 25% (12/48) of the examined cases and represented the most frequently amplified gene. Since the whole-exome analysis was limited to only 48 patients, *SRC* alterations were analyzed *via* FISH in a larger dimension with 135 cases and 217 single samples. This not only intended more accuracy but also to understand the distribution of amplifications among primary tumors and lymph node or distant metastases. The comparison of FISH analysis and WES results (aligned by *SRC*'s chromosomal position) yielded similar amplification rates in both collectives.

3.4.3. Relationship between *SRC* copy number gains and chromosome 18

Since chromosome 18 loss is the most prominent alteration to bear upon SI-NETs, it is worthwhile finding out to which extent it correlates with *SRC* copy number gains. Statistical evaluation pointed out a significant association of these events ($p = 0.027$), at least for primary tumors.

3.4.4. Influence of *SRC* copy number gains on tumor stage

The impact of *SRC* copy numbers on tumor progression was tested for two variables: TNM criteria and UICC stage clusters (encoded 1 accounted for all stages separately, encoded 2 combined stages I-IIB, encoded 3 combined stages I-IIIA, as described in 2.1.). Regarding TNM criteria, there was no evident association with *SRC* signal gains, in none of the examined fractions (primary tumor, metastases and all clinical cases). While statistical analysis did not display a significant connection between *SRC* amplifications and UICC stages for lymph node or distant metastases, primary tumors and all clinical cases (without regard to the metastatic situation) were shown to be significantly influenced by *SRC* amplifications. In all UICC stage clusters *SRC* copy numbers were clearly correlated with tumor progress, which emphasizes that highly enhanced signals were particularly noticed in advanced primary tumors

(p = 0.021 for all stages separately; 0.004 for stages I-IIB versus IIIA, IIIB and IV; 0.032 for stages I-IIIA versus IIIB and IV) and in clinical cases in general (p = 0.004 for all stages separately; < 0.001 for stages I-IIB versus IIIA, IIIB and IV; 0.002 for stages I-IIIA versus IIIB and IV). Table 14 specifies the distribution of amplified cases by UICC tumor stage in primary tumors and all clinical cases. A comparison of *SRC*-amplified and regular samples for all clinical cases is provided for all stages separately in Figure 22 and for a UICC stage cluster (encoded 3) in Figure 23.

Table 14. *SRC* copy number variations in primary tumors and in all clinical cases grouped by tumor stage.

UICC stage	Copy number variations in primary tumors	Copy number variations in all clinical cases
I	0% (0/7)	0% (0/7)
IIA	0% (0/6)	0% (0/6)
IIB	0% (0/5)	0% (0/5)
IIIA	100% (1/1)	100% (1/1)
I – IIIA	5% (1/19)	5% (1/19)
IIIB	11% (4/36)	14% (5/36)
IV	29% (14/49)	39% (22/56)

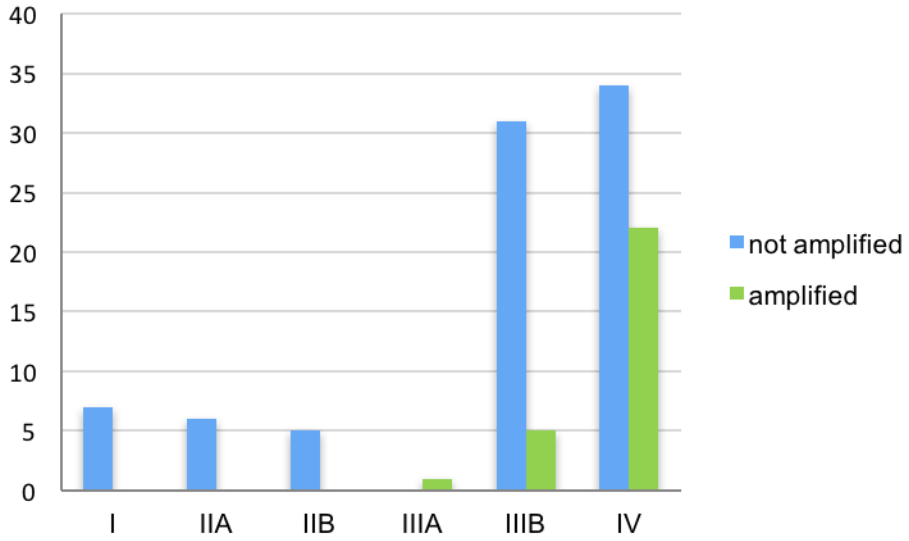

Figure 22. *SRC* copy number variations matching single UICC stages. Not amplified, blue; amplified, green. Clinical cases n = 111, *p* = 0.004.

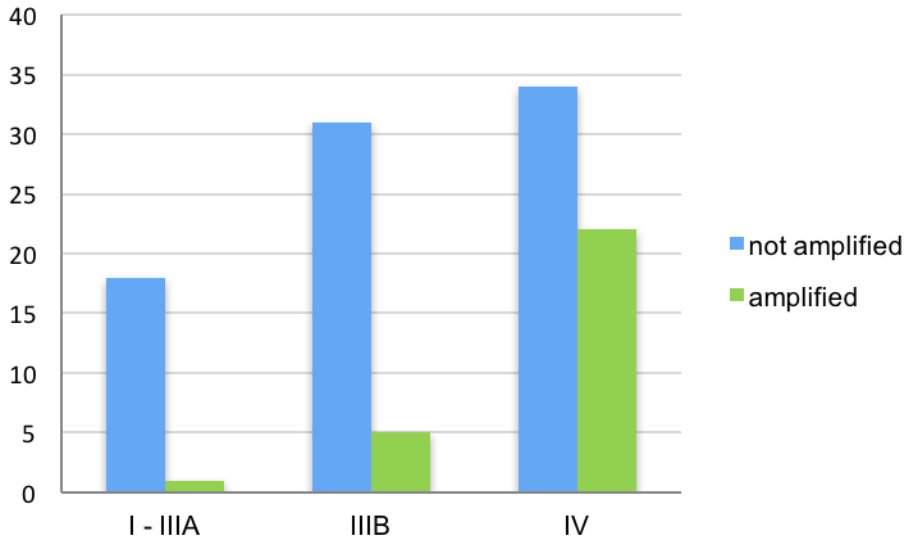

Figure 23. *SRC* copy number variations matching clustered UICC stages. Not amplified, blue; amplified, green. Clinical cases n = 111, *p* = 0.002.

3.4.5. Correlation of *SRC* copy number gains and survival

Whether *SRC* copy number gains have an effect on overall survival was tested for primary tumors and metastases individually and for the clinical cases as a whole. There was no significant association in any of these categories, though. As demonstrated by the Kaplan-Meier curves in Figure 24, the survival functions

of patients with and without *SRC* amplifications have almost identical slopes and terminal points.

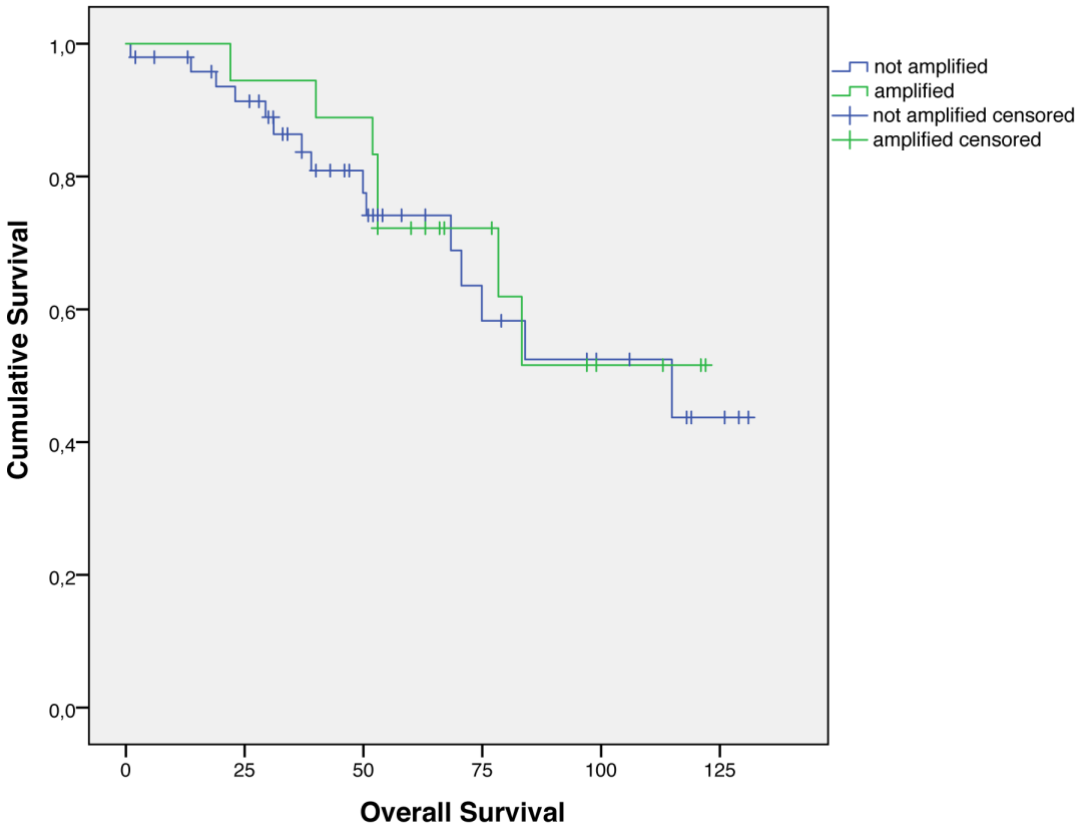

Figure 24. Overall survival represented by Kaplan-Meier curves with and without *SRC* amplifications. Not amplified, blue; amplified, green. Clinical cases n = 67, $p = 0.717$.

3.5. SRC protein expression analyzed by immunohistochemistry

3.5.1. SRC protein expression intensity

SRC expression was examined *via* IHC and evaluated according to both Remmele score and dichotomic division. Figure 25 contrasts the high cytoplasmic SRC expression of a representative immunostained SI-NET sample with its negative nuclear expression. Protein levels were moderate or strong, as defined by Remmele score, in 93% of the primary tumors, 91% of the lymph node metastases and 86% of the distant metastases. Pursuant to dichotomic division,

moderate or strong expression was less frequent with only 49% in primary tumors, 32% in lymph node metastases and 29% in distant metastases, which implies that the major part of the samples featured rather moderate than strong protein expression. These results are summarized in Table 15.

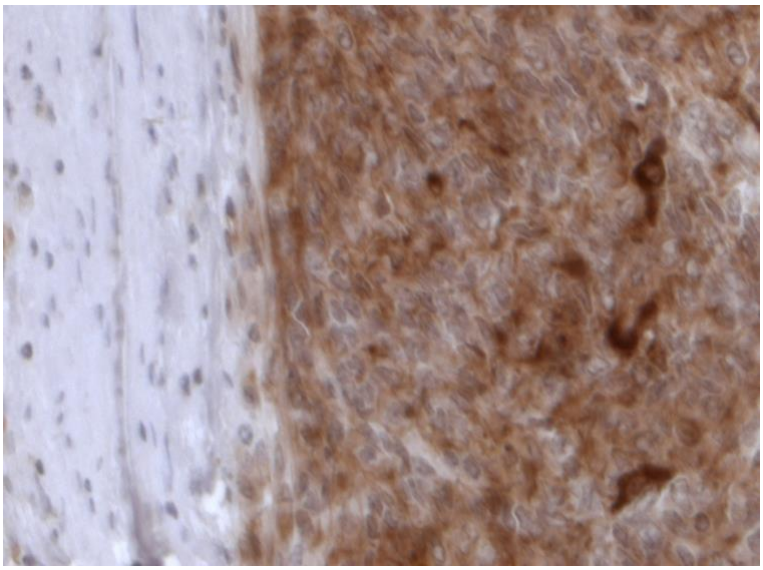

Figure 25. Immunohistochemical SRC staining of an exemplary SI-NET tissue, magnification 400x. High cytoplasmic, no nuclear expression.

Table 15. SRC protein expression. Different staining intensities as a percentage of all applicable cases in primary tumors (P), lymph node metastases (LN), distant metastases (DM) and clinical cases irrespective of spreading progress (Any).

SRC	**Applicable cases**	**0-3 staining** (none / weak)	**4-12 staining** (moderate / strong)	**0-6 staining** (none-moderate)	**7-12 staining** (strong)
P	108	7% (8/108)	93% (100/108)	51% (55/108)	49% (53/108)
LN	68	9% (6/68)	91% (62/68)	68% (46/68)	32% (22/68)
DM	14	14% (2/14)	86% (12/14)	71% (10/14)	29% (4/14)
Any	115	3% (3/115)	97% (112/115)	38% (44/115)	62% (71/115)

The differences of SRC expression in primary tumors and metastases are illustrated based on the Remmele IRS (Figure 26) and on dichotomic distribution (Figure 27).

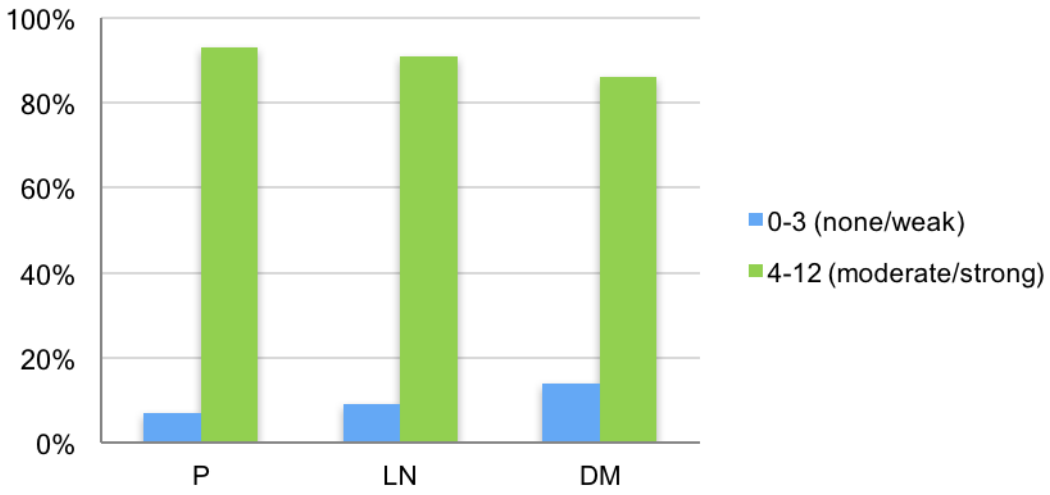

Figure 26. SRC protein expression based on the Remmele IRS in primary tumors (P), lymph node metastases (LN) and distant metastases (DM). None / weak expression, blue; moderate / strong expression, green.

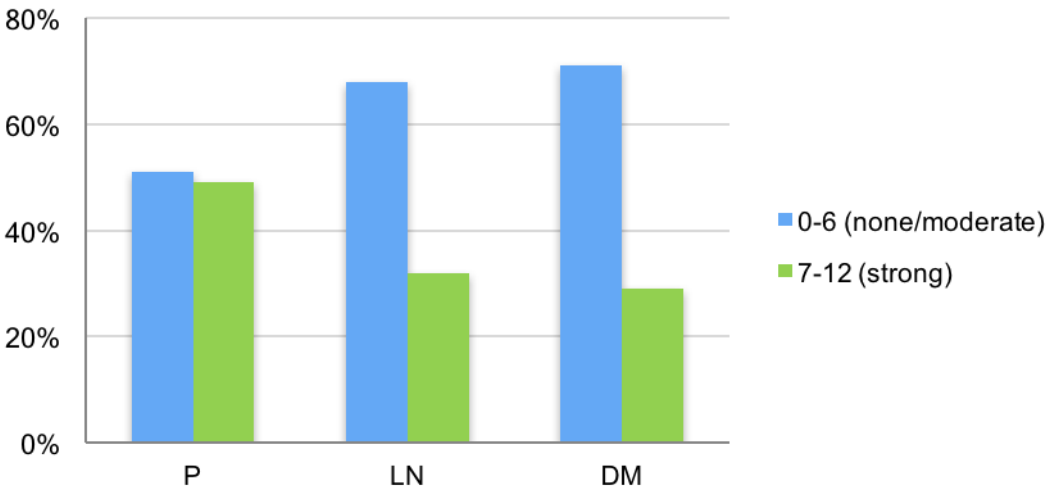

Figure 27. Dichotomic distribution of SRC protein levels in primary tumors (P), lymph node metastases (LN) and distant metastases (DM). None / moderate expression, blue; strong expression, green.

3.5.2. Effect of *SRC* copy number gains on protein expression

Statistical analysis of *SRC* signals compared to SRC expression was performed to figure out the relation of these variables. The testing included matching pairs of FISH signals (amplified versus not amplified) on one hand and protein expression (ascending staining intensity from 0 to 12) on the other for primary tumors, lymph node metastases, distant metastases and clinical cases characterized by any of these (without regard to spread category).

Eventually, there is no evidence of significant correlation of amplified gene signals and protein expression for *SRC*.

3.5.3. Correlation of SRC expression and tumor progress

The impact of SRC expression on tumor progress was tested in primary tumors and metastases separately and in all clinical cases combined. For this purpose, SRC levels were correlated with TNM criteria and UICC stages (clustered as encoded 1, 2 and 3). Statistic results did not identify a connection between Src kinase expression and T or N stages in any constellation. Yet, primary tumors ($p = 0.043$) and clinical cases in general (subject to Remmele score evaluation, $p = 0.001$) presented significantly high Src kinase levels in M stage. The comparison of SRC expression in distinct UICC stages yielded significantly high levels in lymph node samples of advanced stages (same p of 0.039 for all stages separately, for stages I-IIB opposite to IIIA, IIIB and IV and for stages I-IIIA opposite to IIIB and IV). However, this was not evident in primary tumors, distant metastases or clinical cases in general.

4. Discussion

Neuroendocrine tissue scattered over several organs can give rise to heterogeneous tumors. In the small intestine, these neuroendocrine tumors are the leading malignancy. Since the majority is diagnosed when already spread, most patients do not benefit from surgery which is the only curative treatment so far. A potential target for innovative therapy could the molecular background of SI-NETs.

A sequencing study conducted by Banck *et al.* in 2013 disclosed amplifications of two genes, located on chromosome 20: *AURKA* and *SRC*.[28] Prior to this, amplification and overexpression of both genes / proteins have been identified in many other cancer types. Elevated protein levels of the mitotic regulator AURKA is considered to cause irregular centrosome multiplication and spindle arrangement resulting in aneuploidy. SRC protein excess seems to support tumor invasion and dissemination stimulated by its downstream pathways.

The present study focused on the identification of AURKA and SRC alterations in SI-NETs. While gene signals were registered by fluorescence *in situ* hybridization, protein expression was analyzed *via* immunohistochemistry. 135 patients providing 217 tissue samples arranged as tissue microarrays were taken into account.

Signal counts revealed *AURKA* gains in 24% and *SRC* gains in 25% of the investigated tumor samples. These results are consistent with the amplification rates provided by Banck *et al.*[28] FISH analysis yielded slightly higher copy number gains for both genes compared to the sequencing study. Considering the ratios of gene signal to calculated centromere signal, the attested copy number gains are largely characterized by chromosome 20 polysomy. Only a small fraction (7% for *AURKA* and 4% for *SRC*) could be attributed to specific gene amplifications. Toennies *et al.* verified chromosomal arm gains of 20q as frequent alteration (36%) in NETs of the midgut.[22] In this context, it is plausible that amplifications of larger chromosomal segments including the locations of *AURKA* and *SRC* (20q11.23 – 20q13.2) account for the identified signal increase.

A comparative analysis matched the FISH results against the NGS findings by Banck *et al.* for both genes. 25% of the cases evaluated as augmented by FISH featured corresponding gains of larger chromosomal regions which were rated as amplified by NGS. Apparently, the sequencing results are also based on polysomy.

This investigation provided additional information about genetic properties of SI-NET metastases. *AURKA* gains were distributed equally in metastases and primary tumors, whereas *SRC* gains most of all manifested in lymph node and distant metastases.

Given the fact that primary tumors with loss of chromosome 18 displayed enhanced *AURKA* and *SRC* signals (p = 0.028 and 0.027, respectively), the question arises how these events relate to each other. In metastases, there was no evident relationship between these events but in early tumors, there was a significant correlation between loss of chromosome 18 and increased *AURKA* and *SRC* copy numbers. This is compliant with loss of chromosome 18 being considered an early event in tumor development.[25] Chromosome 18 loss correlating with *AURKA* / *SRC* increases due to chromosome 20 gains corresponds with several chromosomal interdependencies outlined by Francis *et al.*[29] A potential reason for this coexistence could be passenger chromosomal instability caused by loss of chromosome 18.

Despite the lack of a significant effect on TNM criteria, *AURKA* and *SRC* copy number gains were significantly connected to advanced UICC stages. In particular, signals were higher in patients with advanced (UICC stage IIIB and IV) tumors (p = 0.020 for *AURKA*, p = 0.002 for *SRC*). This highlights the influence of *AURKA* and *SRC* copy number alterations on tumor progression. Assuming that chromosomal gains comprising *AURKA* and *SRC* are side effects of other driving events (such as chromosome 18 loss) they may play a minor role in primary tumor emergence but apparently promote invasion and dissemination.

Overall survival of SI-NET patients did not noticeably depend on *AURKA* or *SRC* copy number gains, even though facilitated tumor spread clearly reduces the chance of survival. This can be explained by the late tumor manifestation and

diagnosis. Regardless of *AURKA* or *SRC* gene levels, SI-NETs are commonly identified in a metastatic state and are thus fatal. The long period of undetected tumor persistence makes it difficult to correlate underlying events and survival.

In 78% of the considered cases, AURKA protein expression reached medium to high levels. There were generally higher levels in the nuclear than in the cytoplasmic compartment. At the same time, nuclear and cytoplasmic levels were significantly aligned in clinical cases, regardless of metastatic spread ($p = 0.042$). In other words, the higher the nuclear AURKA expression, the higher the cytoplasmic expression in the same patient. In both cell compartments, Aurora A expression was more intense in primary tumors than in metastases. Remarkably, distant metastases largely presented negative nuclei. Due to its predominance in primary tumors, nuclear Aurora A excess could be involved in the emergence of SI-NETs. This is plausible with Aurora's regulatory function in mitosis but stands in contrast with the effect of *AURKA* copy number gains (considered to assist tumor spread).

SRC expression was moderately high in 97% and very intensive in 62% of the examined cases. High levels, in particular, were more frequent in primary tumors than in metastases (49% versus 32% in lymph node and 29% in distant metastases, respectively). This is a surprising result because *SRC* copy number gains were demonstrated to determine advanced tumor stages with significant increase in metastases. Additionally, *SRC* proto-oncogene in other tumors turned out to control invasion and tumor spread and hence was more expected to assist tumor progress than tumor formation.[62]

Catalytic activity was tested with antibodies targeting phosphorylation site Thr_{288} for AURKA and Tyr_{527} for SRC. However, due to irregular staining, the results could not be evaluated.

Amplified gene signals did not seem to have an influence on the expression level of encoded proteins, neither in the case of *AURKA*, nor in the case of *SRC*. This leads to the assumption that in the investigated SI-NETs, protein expression was not intensified by genetic variations but by other mechanisms. Since phosphorylation is a key regulator of both genes dysfunctional protein kinase

activity could lead to AURKA and SRC excess.[38,58] Even though several studies found coincidence of amplification and overexpression, high AURKA mRNA and protein expression were also found without copy number gains in solid cancers.[40,41] In particular, transcriptional activation, (post-)translational up-regulation and reduced degradation were reported as a cause of overexpression.[43,85,86] In cells exposed to hypoxia such as tumor cells, HIF-1-induced gene transcription lead to AURKA excess.[87] In EGFR-overexpressing cancer cell lines AURKA levels were shown to increase due to EGF-stimulation in various ways: nuclear EGF signaling acted as transcriptional activator and enhanced STAT5-mediated AURKA expression.[88] Additionally, EGF downstream protein mTOR raised translational efficiency of AURKA mRNA and specific splicing variants were associated with higher protein expression.[89] SRC protein levels in most cancers are mainly affected by (epi-)genetic alterations.[90] Increased SRC expression, however, was also ascribed to enhanced transcription in colon cancer cell lines and to deficient inhibitory phosphorylation in hepatocellular carcinoma.[60,91] EGF signaling not only affects AURKA but has also an impact on SRC protein levels, which was studied in human breast cancer cell lines. EGFR-member HER2 generated SRC up-regulation by activating downstream protein mTOR which intensified SRC translation.[92] Biscardi *et al.* identified a mutually potentiating interaction between SRC and HER1.[93] Since EGF-signaling plays an important role in both AURKA and SRC synthesis and amplifications of all three genes have been detected in SI-NETs protein interactions like these could explain overexpression independent of gene copy numbers in the analyzed tumor samples.

This study provides an insight into molecular modifications in SI-NETs taking advantage of both target genes being located on chromosome 20. This compensated for the bias of single person evaluation. A similar effect was achieved by comparing immunohistochemistry stainings with the corresponding Definiens Tissue Studio extrapolation. The quantity of investigated patients and samples in this study was considerably higher than in the previous study by Banck *et al.* but especially for the newly acquired knowledge about the genetics and protein expression of distant metastases, the small number of samples

should be taken into account. Little sample supply due to a low incidence, however, is rated as general obstacle in exploring SI-NETs.[27] In order to provide a better understanding of this rare malignancy, a higher detection rate is indispensable. Diagnostics could be improved by polymerase chain reaction (PCR) based tumor cell analysis in serum, as introduced by Modlin *et al.* Due to higher sensitivity and specificity this method could replace current blood tests.[94] However, this would only confirm a suspected diagnosis and would not have an impact on patients without symptoms. Therefore, early SI-NET identification requires viable and inexpensive screening tools.

In conclusion, *AURKA* signal gains were evident in 24% and *SRC* gains in 25% of the studied cases. Protein expression was considerably high in 78% for AURKA and 62% for SRC. In this way, previous findings were confirmed and supplemented by additional methods based on a larger case quantity. Increased gene signals (predominantly) turned out to be gains of major parts of chromosome 20, rather than specific gene amplifications. The discrepancy between the distribution patterns of primary tumors and metastases indicates a different influence of molecular and protein alterations on tumor emergence and dissemination. Protein overexpression has been pointed out as largely independent of gene copy number gains. Yet, both mechanisms seem to play a significant role in SI-NET development.

Therefore, targeting these proteins with inhibitory agents in clinical studies could be profitable. Potential candidate agents include the AURKA inhibitors Alisertib or Danusertib and the SRC inhibitors Bosutinib or Dasatinib.

Since AURKA and SRC are subject to similar regulation with complementary functions in tumorigenesis, the idea of dual protein inhibition came up. Ratushny *et al.* proved AURKA and SRC interactions in colorectal and ovarian cancer and achieved tumor cell death by simultaneously blocking both *in vitro*.[95] In consequence, synergetic effects of AURKA and SRC are interesting issues to be further pursued.

5. Summary

Neuroendocrine Tumors (NETs) are rare neoplasias of hormone-producing cells largely emerging from the gastroenteropancreatic system.[2] They represent the leading malignancy of the small intestine.[6] Due to their long asymptomatic progression SI-NETs are diagnosed late and most commonly in a metastatic stage. This limits the feasibility of radical surgery, the only curative therapy. Aside from local procedures to reduce tumor load somatostatin analogs and interferons are applied for symptomatic treatment. The development of specific immunotherapy requires an understanding of causal genetic modifications. Loss of chromosome 18 is an early event in cancer development and is thus considered the most important finding in gastrointestinal NETs.[21-25] Based on comparative genomic hybridization (CGH) analyses determining further chromosomal alterations, Banck *et al.* conducted a whole exome sequencing (WES) study using SI-NET samples of 48 patients. They confirmed several amplifications including chromosome 20 and associated genes that facilitate enhanced cell growth and reduced apoptosis, such as *AURKA* and *SRC*.[28]

This thesis is focused on fluorescence *in situ* hybridization (FISH) analysis of these two genes and provides insight into their protein expression *via* immunohistochemistry. Comprising 217 SI-NET samples of 135 patients the study is fairly representative.

Both genes were characterized by signal gains. *AURKA* gains were demonstrated in 24% and *SRC* gains in 25% of the studied cases in accordance with the results of Banck *et al*.[28] FISH attested slightly higher copy numbers compared to sequencing. For the most part these gains are ascribed to amplification of major chromosomal segments (polysomy) but a few samples also featured specific gene amplifications. Moreover, this analysis yielded a distribution pattern of copy number gains between primary tumor and metastases. A significant correlation between copy number gains in primary tumors and loss of chromosome 18 was demonstrated for *AURKA* and *SRC* (*p*-value: 0.028 for *AURKA* and 0.027 for *SRC*). Since particularly high copy numbers were most notably detected in advanced tumors in UICC stages IIIB

and IV (*p*-value: 0.020 for *AURKA* and 0.002 for *SRC*) these alterations are most likely related to tumor invasion and dissemination.

Protein analysis proved medium to high expression in 78% for AURKA and 97% for SRC. There were considerably higher levels of both proteins in primary tumors than in metastases. In contrast to their encoding genes, AURKA and SRC seem to be more involved in tumor emergence than in spreading.

Even though increased expression at molecular and protein levels are both factors in SI-NET growth, there is no direct interrelation of these two. Instead, elevated protein levels potentially result from intensified transcription, translational up-regulation or reduced degradation.[43,85,86] In this context, the EGF-signaling pathway plays an important role in the control of both proteins.[88,89,92]

AURKA / SRC have already been targeted by inhibitory agents such as AURKA inhibitors Alisertib or Danusertib and SRC inhibitors Bosutinib or Dasatinib in several cancer types. Future studies could therefore test these candidates for immunotherapy in non-resectable SI-NETs.

6. Zusammenfassung

Neuroendokrine Tumoren (NETs) sind seltene, von hormonproduzierenden Zellen ausgehende Neoplasien, die zum größten Teil im gastroenteropankreatischen System entstehen.[2] Im Dünndarm stellen sie die häufigste maligne Entartung dar.[6] Aufgrund ihres langen asymptomatischen Verlaufs werden sie spät und meist im metastasierten Zustand diagnostiziert. Dies begrenzt die Möglichkeit einer chirurgischen Radikalresektion, der einzig kurativen Therapie. Abgesehen von lokalen Maßnahmen zur Reduktion der Tumorlast werden systemisch Somatostatin-Analoga und Interferone zur symptomatischen Behandlung eingesetzt. Voraussetzung für die Entwicklung spezifischer Immuntherapeutika ist das Verständnis zugrundeliegender genetischer Veränderungen. Der Verlust von Chromosom 18 ist ein frühes Ereignis während der Tumorentwicklung und gilt als wichtigste Erkenntnis im Rahmen gastrointestinaler NETs.[21-25] Ausgehend von Comparative genomic hybridization (CGH) Analysen, mit deren Hilfe weitere Chromosomenveränderungen festgestellt wurden, führten Banck *et al.* eine Whole exome sequencing (WES) Studie anhand SI-NETs von 48 Patienten durch. Dabei wurde unter anderem die Amplifikation von Chromosom 20 untermauert, sowie Amplifikationen assoziierter Gene, die vermehrtes Wachstum oder verminderte Apoptose begünstigen, wie beispielsweise *AURKA* und *SRC*.[28]

Die vorliegende Arbeit konzentriert sich auf die Analyse dieser zwei Gene mittels Fluoreszenz *in situ* Hybridisierung (FISH) sowie der Proteinprodukte anhand Immunhistochemie. Diese Untersuchung umfasst 217 SI-NET Proben von 135 Patienten und ist verhältnismäßig repräsentativ.

Beide Gene wiesen vermehrte Signale auf. *AURKA* war in 24% und *SRC* in 25% der Fälle vervielfältigt, was mit den Ergebnissen von Banck *et al.* übereinstimmt.[28] Mittels FISH wurde im Vergleich zur Sequenzierung jeweils eine geringfügig höhere Anzahl an Genkopien nachgewiesen. Zum größten Teil handelt es sich hierbei um die Vervielfältigung größerer Chromosomenabschnitte (Polysomie), aber einzelne Fälle zeigten auch Amplifikationen spezifischer

Gensignale. Darüber hinaus lieferte diese Untersuchung ein Verteilungsmuster der vermehrten Gensignale zwischen Primärtumoren und Metastasen. Eine Korrelation zwischen erhöhten Genkopien und dem Verlust von Chromosom 18 wurde für *AURKA* und *SRC* festgestellt (*p*-Wert: 0,028 für *AURKA* und 0,027 für *SRC*). Da erhöhte Gensignale vor allem in weit fortgeschrittenen Tumoren der UICC Stadien IIIB und IV (*p*-Wert: 0,020 für *AURKA* und 0,002 für *SRC*) vorlagen, ist ein Zusammenhang mit Tumorinvasion und Metastasierung wahrscheinlich.

Auf Proteinebene zeigte sich in 78% der Fälle für AURKA und in 97% für SRC eine moderate bis starke Expression. Primärtumoren waren durch ein deutlich höheres Expressionsniveau beider Proteine gekennzeichnet als Metastasen. Im Gegensatz zu den kodierenden Genen scheinen AURKA und SRC eher an der Tumorentstehung als an der Metastasierung beteiligt zu sein.

Obwohl eine verstärkte Expression sowohl auf molekularer als auch auf Proteinebene Einfluss auf die SI-NET Entwicklung hat, gibt es in diesem Fall keine direkte Wechselwirkung. Vielmehr könnte die erhöhte Proteinexpression eine Folge von verstärkter Transkription, Hochregulierung der Translation oder vermindertem Abbau sein.[43,85,86] Der EGF-Signalweg spielt bei der Regulierung beider Proteine eine wichtige Rolle.[88,89,92]

Bei einigen Krebsarten wurden die AURKA Inhibitoren Alisertib oder Danusertib und SRC Inhibitoren Bosutinib oder Dasatinib bereits zur AURKA / SRC Antagonisierung eingesetzt. Zukünftige Studien könnten daher diese Substanzen in nicht resektablen SI-NETs untersuchen.

7. References

[1] Hauso, O.; Gustafsson, B. I.; Kidd, M.; Waldum, H. L.; Drozdov, I.; Chan, A. K.; Modlin, I. M. Neuroendocrine tumor epidemiology, *Cancer* **2008**, *113*, 2655-2664.

[2] Modlin, I. M.; Sandor, A. An analysis of 8305 cases of carcinoid tumors, *Cancer* **1997**, *79*, 813-829.

[3] Kaltsas, G. A.; Besser, G. M.; Grossman, A. B. The diagnosis and medical management of advanced neuroendocrine tumors, *Endocrine Reviews* **2004**, *25*, 458-511.

[4] Yao, J. C.; Hassan, M.; Phan, A.; Dagohoy, C.; Leary, C.; Mares, J. E.; Abdalla, E. K.; Fleming, J. B.; Vauthey, J.-N.; Rashid, A.; Evans, D. B. One hundred years after “carcinoid”: epidemiology of and prognostic factors for neuroendocrine tumors in 35,825 cases in the United States, *Journal of Clinical Oncology* **2008**, *26*, 3063-3072.

[5] Klimstra, D. S.; Modlin, I. R.; Coppola, D.; Lloyd, R. V.; Suster, S. The pathologic classification of neuroendocrine tumors: a review of nomenclature, grading, and staging systems, *Pancreas* **2010**, *39*, 707-712.

[6] Banck, M. S.; Beutler, A. S. Advances in small bowel neuroendocrine neoplasia, *Current Opinion in Gastroenterology* **2014**, *30*, 163-167.

[7] Niederle, B. *et al.* ENETS consensus guidelines update for neuroendocrine neoplasms of the jejunum and ileum, *Neuroendocrinology* **2016**, *103*, 125-138.

[8] Hamilton, S. R.; Aaltonen, L. A. *World Health Organization classification of tumours. Pathology and genetics of tumours of the digestive system*. IARC Press: Lyon **2000**, 48.

[9] Cunningham, J. L.; Díaz de Ståhl, T.; Sjöblom, T.; Westin, G.; Dumanski, J. P.; Janson, E. T. Common pathogenetic mechanism involving human chromosome 18 in familial and sporadic ileal carcinoid tumors, *Genes, Chromosomes and Cancer* **2011**, *50*, 82-94.

[10] Mawe, G. M.; Hoffman, J. M. Serotonin signalling in the gut - functions, dysfunctions and therapeutic targets, *Nature Reviews Gastroenterology & Hepatology* **2013**, *10*, 473-486.

[11] Turaga, K. K.; Kvols, L. K. Recent progress in the understanding, diagnosis, and treatment of gastroenteropancreatic neuroendocrine tumors, *CA: A Cancer Journal for Clinicians* **2011**, *61*, 113-132.

[12] Bosman, F. T.; Carneiro, F.; Hruban, R. H.; Theise, N. D. *WHO Classification of Tumours of the Digestive System, 4th edition*. IARC Press: Lyon **2010**.

[13] Rindi, G.; Wiedenmann, B. Neuroendocrine neoplasms of the gut and pancreas: new insights, *Nature Reviews Endocrinology* **2012**, *8*, 54-64.

[14] Niederle, M. B.; Hackl, M.; Kaserer, K.; Niederle, B. Gastroenteropancreatic neuroendocrine tumours: the current incidence and staging based on the WHO and European Neuroendocrine Tumour Society classification: an analysis based on prospectively collected parameters, *Endocrine-Related Cancer* **2010**, *17*, 909-918.

[15] Kidd, M.; Modlin, I. M. Small intestinal neuroendocrine cell pathobiology: ‘carcinoid’ tumors, *Current Opinion in Oncology* **2011**, *23*, 45-52.
[16] Tomassetti, P.; Migliori, M.; Lalli, S.; Campana, D.; Tomassetti, V.; Corinaldesi, R. Epidemiology, clinical features and diagnosis of gastroenteropancreatic endocrine tumours, *Annals of Oncology* **2001**, *12*, S95-S99.
[17] Ramage, J. K. *et al.* Guidelines for the management of gastroenteropancreatic neuroendocrine (including carcinoid) tumours (NETs), *Gut* **2012**, *61*, 6-32.
[18] Woodbridge, L. R.; Murtagh, B. M.; Yu, D. F. Q. C.; Planche, K. L. Midgut neuroendocrine tumors: imaging assessment for surgical resection, *RadioGraphics* **2014**, *34*, 413-426.
[19] Capurso, G.; Rinzivillo, M.; Bettini, R.; Boninsegna, L.; Fave, G. D.; Falconi, M. Systematic review of resection of primary midgut carcinoid tumour in patients with unresectable liver metastases, *British Journal of Surgery* **2012**, *99*, 1480-1486.
[20] Lengauer, C.; Kinzler, K. W.; Vogelstein, B. Genetic instabilities in human cancers, *Nature* **1998**, *396*, 643-649.
[21] Terris, B.; Meddeb, M.; Marchio, A.; Danglot, G.; Fléjou, J. F.; Belghiti, J.; Ruszniewski, P.; Bernheim, A. Comparative genomic hybridization analysis of sporadic neuroendocrine tumors of the digestive system, *Genes, Chromosomes and Cancer* **1998**, *22*, 50-56.
[22] Tönnies, H.; Toliat, M.; Ramel, C.; Pape, U.; Neitzel, H.; Berger, W.; Wiedenmann, B. Analysis of sporadic neuroendocrine tumours of the enteropancreatic system by comparative genomic hybridisation, *Gut* **2001**, *48*, 536-541.
[23] Speel, E. J.; Richter, J.; Moch, H.; Egenter, C.; Saremaslani, P.; Rütimann, K.; Zhao, J.; Barghorn, A.; Roth, J.; Heitz, P. U.; Komminoth, P. Genetic differences in endocrine pancreatic tumor subtypes detected by comparative genomic hybridization, *Endocrine* **1999**, *155*, 1787-1794.
[24] Zhao, J.; de Krijger, R. R.; Meier, D.; Speel, E.-J. M.; Saremaslani, P.; Muletta-Feurer, S.; Matter, C.; Roth, J.; Heitz, P. U.; Komminoth, P. Genomic alterations in well-differentiated gastrointestinal and bronchial neuroendocrine tumors (carcinoids): marked differences indicating diversity in molecular pathogenesis, *The American Journal of Pathology* **2000**, *157*, 1431-1438.
[25] Kytölä, S.; Höög, A.; Nord, B.; Cedermark, B.; Frisk, T.; Larsson, C.; Kjellman, M. Comparative genomic hybridization identifies loss of 18q22-qter as an early and specific event in tumorigenesis of midgut carcinoids, *The American Journal of Pathology* **2001**, *158*, 1803-1808.
[26] Zikusoka, M. N.; Kidd, M.; Eick, G.; Latich, I.; Modlin, I. M. The molecular genetics of gastroenteropancreatic neuroendocrine tumors, *Cancer* **2005**, *104*, 2292-2309.
[27] Löllgen, R.-M.; Hessman, O.; Szabo, E.; Westin, G.; Åkerström, G. Chromosome 18 deletions are common events in classical midgut carcinoid tumors, *International Journal of Cancer* **2001**, *92*, 812-815.

[28] Banck, M. S. *et al.* The genomic landscape of small intestine neuroendocrine tumors, *The Journal of Clinical Investigation* **2013**, *123*, 2502-2508.
[29] Francis, J. M. *et al.* Somatic mutation of CDKN1B in small intestine neuroendocrine tumors, *Nature Genetics* **2013**, *45*, 1483-1486.
[30] Kulke, M. H.; Freed, E.; Chiang, D. Y.; Philips, J.; Zahrieh, D.; Glickman, J. N.; Shivdasani, R. A. High-resolution analysis of genetic alterations in small bowel carcinoid tumors reveals areas of recurrent amplification and loss, *Genes, Chromosomes and Cancer* **2008**, *47*, 591-603.
[31] Dreijerink, K. M.; Derks, J. L.; Cataldo, I.; Scarpa, A.; Valk, G. D.; Speel, E.-J. Genetics and epigenetics of pancreatic neuroendocrine tumors and pulmonary carcinoids. *Frontiers of Hormone Research* **2015**, *44*, 115-138.
[32] Jiao, Y. *et al.* DAXX/ATRX, MEN1, and mTOR pathway genes are frequently altered in pancreatic neuroendocrine tumors, *Science* **2011**, *331*, 1199-1203.
[33] Heaphy, C. M. *et al.* Altered telomeres in tumors with ATRX and DAXX mutations, *Science* **2011**, *333*, 425.
[34] Walch, A. K.; Zitzelsberger, H. F.; Aubele, M. M.; Mattis, A. E.; Bauchinger, M.; Candidus, S.; Präuer, H. W.; Werner, M.; Höfler, H. Typical and atypical carcinoid tumors of the lung are characterized by 11q deletions as detected by comparative genomic hybridization, *The American Journal of Pathology* **1998**, *153*, 1089-1098.
[35] Debelenko, L. V. *et al.* Identification of MEN1 gene mutations in sporadic carcinoid tumors of the lung, *Human Molecular Genetics* **1997**, *6*, 2285-2290.
[36] Swarts, D. R.; Scarpa, A.; Corbo, V.; Van Criekinge, W.; Van Engeland, M.; Gatti, G.; Henfling, M. E.; Papotti, M.; Perren, A.; Ramaekers, F. C.; Speel, E. J.; Volante, M. MEN1 gene mutation and reduced expression are associated with poor prognosis in pulmonary carcinoids, *The Journal of Clinical Endocrinology & Metabolism* **2013**, *99*, E374-E378.
[37] Honda, K.; Mihara, H.; Kato, Y.; Yamaguchi, A.; Tanaka, H.; Yasuda, H.; Furukawa, K.; Urano, T. Degradation of human Aurora2 protein kinase by the anaphase-promoting complex-ubiquitin-proteasome pathway, *Oncogene* **2000**, *19*, 2812.
[38] Carmena, M.; Earnshaw, W. C. The cellular geography of Aurora kinases, *Nature Reviews Molecular Cell Biology* **2003**, *4*, 842-854.
[39] Bischoff, J. R.; Anderson, L.; Zhu, Y.; Mossie, K.; Ng, L.; Souza, B.; Schryver, B.; Flanagan, P.; Clairvoyant, F.; Ginther, C.; Chan, C. S.; Novotny, M.; Slamon, D. J.; Plowman, G. D. A homologue of Drosophila Aurora kinase is oncogenic and amplified in human colorectal cancers, *The EMBO Journal* **1998**, *17*, 3052-3065.
[40] Zhou, H.; Kuang, J.; Zhong, L.; Kuo, W.-l.; Gray, J. W.; Sahin, A.; Brinkley, B. R.; Sen, S. Tumour amplified kinase STK15/BTAK induces centrosome amplification, aneuploidy and transformation, *Nature Genetics* **1998**, *20*, 189.
[41] Sakakura, C.; Hagiwara, A.; Yasuoka, R.; Fujita, Y.; Nakanishi, M.; Masuda, K.; Shimomura, K.; Nakamura, Y.; Inazawa, J.; Abe, T.;

Yamagishi, H. Tumour-amplified kinase BTAK is amplified and overexpressed in gastric cancers with possible involvement in aneuploid formation, *British Journal of Cancer* **2001**, *84*, 824.

[42] Crane, R.; Gadea, B.; Littlepage, L.; Wu, H.; Ruderman, J. V. Aurora A, meiosis and mitosis, *Biology of the Cell* **2004**, *96*, 215-229.

[43] Nikonova, A. S.; Astsaturov, I.; Serebriiskii, I. G.; Dunbrack, R. L.; Golemis, E. A. Aurora A kinase (AURKA) in normal and pathological cell division, *Cellular and Molecular Life Sciences* **2013**, *70*, 661-687.

[44] Sun, J.-M.; Yang, L.-N.; Xu, H.; Chang, B.; Wang, H.-Y.; Yang, G. Inhibition of Aurora A promotes chemosensitivity via inducing cell cycle arrest and apoptosis in cervical cancer cells, *American Journal of Cancer Research* **2015**, *5*, 1133-1145.

[45] Warner, S. L.; Bearss, D. J.; Han, H.; Von Hoff, D. D. Targeting Aurora-2 kinase in cancer, *Molecular Cancer Therapeutics* **2003**, *2*, 589-595.

[46] Anand, S.; Penrhyn-Lowe, S.; Venkitaraman, A. R. AURORA-A amplification overrides the mitotic spindle assembly checkpoint, inducing resistance to Taxol, *Cancer Cell* **2003**, *3*, 51-62.

[47] Katayama, H.; Sasai, K.; Kawai, H.; Yuan, Z.-M.; Bondaruk, J.; Suzuki, F.; Fujii, S.; Arlinghaus, R. B.; Czerniak, B. A.; Sen, S. Phosphorylation by Aurora kinase A induces Mdm2-mediated destabilization and inhibition of p53, *Nature Genetics* **2004**, *36*, 55-62.

[48] Mehra, R.; Serebriiskii, I. G.; Burtness, B.; Astsaturov, I.; Golemis, E. A. Aurora kinases in head and neck cancer, *The Lancet Oncology* **2013**, *14*, 425-435.

[49] Dar, A. A.; Goff, L. W.; Majid, S.; Berlin, J.; El-Rifai, W. Aurora kinase inhibitors - rising stars in cancer therapeutics? *Molecular Cancer Therapeutics* **2010**, *9*, 268-278.

[50] Fraedrich, K.; Schrader, J.; Ittrich, H.; Keller, G.; Gontarewicz, A.; Matzat, V.; Kromminga, A.; Pace, A.; Moll, J.; Bläker, M.; Lohse, A. W.; Hörsch, D.; Brümmendorf, T. H.; Benten, D. Targeting aurora kinases with danusertib (PHA-739358) inhibits growth of liver metastases from gastroenteropancreatic neuroendocrine tumors in an orthotopic xenograft model, *Clinical Cancer Research* **2012**, *18*, 4621-4632.

[51] Michael Bishop, J. Enemies within: the genesis of retrovirus oncogenes, *Cell* **1981**, *23*, 5-6.

[52] Bishop, J. M. Retroviruses and cancer genes, *Advances in Cancer Research* **1982**, *37*, 1-32.

[53] Uhlén, M. *et al.* Tissue-based map of the human proteome, *Science* **2015**, *347,* 1260419.

[54] Uhlen, M.; Oksvold, P.; Fagerberg, L.; Lundberg, E.; Jonasson, K.; Forsberg, M.; Zwahlen, M.; Kampf, C.; Wester, K.; Hober, S.; Wernerus, H.; Bjorling, L.; Ponten, F. Towards a knowledge-based human protein atlas, *Nature Biotechnology* **2010**, *28*, 1248-1250.

[55] Martin, G. S. The hunting of the Src, *Nature Reviews Molecular Cell Biology* **2001**, *2*, 467-475.

[56] Thomas, S. M.; Brugge, J. S. Cellular functions regulated by Src family kinases, *Annual Review of Cell and Developmental Biology* **1997**, *13*, 513-609.

[57] Ishizawar, R.; Parsons, S. J. C-Src and cooperating partners in human cancer, *Cancer Cell* **2004**, *6*, 209-214.
[58] Boggon, T. J.; Eck, M. J. Structure and regulation of Src family kinases, *Oncogene* **2004**, *23*, 7918-7927.
[59] Wheeler, D. L.; Iida, M.; Dunn, E. F. The role of Src in solid tumors, *The Oncologist* **2009**, *14*, 667-678.
[60] Masaki, T.; Okada, M.; Tokuda, M.; Shiratori, Y.; Hatase, O.; Shirai, M.; Nishioka, M.; Omata, M. Reduced C-terminal Src kinase (Csk) activities in hepatocellular carcinoma, *Hepatology* **1999**, *29*, 379-384.
[61] Irby, R. B.; Mao, W.; Coppola, D.; Kang, J.; Loubeau, J. M.; Trudeau, W.; Karl, R.; Fujita, D. J.; Jove, R.; Yeatman, T. J. Activating SRC mutation in a subset of advanced human colon cancers, *Nature Genetics* **1999**, *21*, 187-190.
[62] Frame, M. C. Src in cancer: deregulation and consequences for cell behaviour, *Biochimica et Biophysica Acta (BBA) - Reviews on Cancer* **2002**, *1602*, 114-130.
[63] Luttrell, D.; Luttrell, L.; Parsons, S. Augmented mitogenic responsiveness to epidermal growth factor in murine fibroblasts that overexpress pp60c-src, *Molecular and Cellular Biology* **1988**, *8*, 497-501.
[64] Sieg, D. J.; Hauck, C. R.; Ilic, D.; Klingbeil, C. K.; Schaefer, E.; Damsky, C. H.; Schlaepfer, D. D. FAK integrates growth-factor and integrin signals to promote cell migration, *Nature Cell Biology* **2000**, *2*, 249-256.
[65] Rodier, J.-M.; Vallés, A. M.; Denoyelle, M.; Thiery, J. P.; Boyer, B. Pp60c-src is a positive regulator of growth factor-induced cell scattering in a rat bladder carcinoma cell line, *The Journal of Cell Biology* **1995**, *131*, 761-773.
[66] Behrens, J.; Vakaet, L.; Friis, R.; Winterhager, E.; Van Roy, F.; Mareel, M. M.; Birchmeier, W. Loss of epithelial differentiation and gain of invasiveness correlates with tyrosine phosphorylation of the E-cadherin/beta-catenin complex in cells transformed with a temperature-sensitive v-SRC gene, *Journal of Cell Biology* **1993**, *120*, 757-766.
[67] Guarino, M. Src signaling in cancer invasion, *Journal of Cellular Physiology* **2010**, *223*, 14-26.
[68] Lombardo, L. J. *et al.* Discovery of N-(2-chloro-6-methyl-phenyl)-2-(6-(4-(2-hydroxyethyl)-piperazin-1-yl)-2-methylpyrimidin-4-ylamino) thiazole-5-carboxamide (BMS-354825), a dual Src/Abl kinase inhibitor with potent antitumor activity in preclinical assays, *Journal of Medicinal Chemistry* **2004**, *47*, 6658-6661.
[69] Nam, S.; Kim, D.; Cheng, J. Q.; Zhang, S.; Lee, J.-H.; Buettner, R.; Mirosevich, J.; Lee, F. Y.; Jove, R. Action of the Src family kinase inhibitor, dasatinib (BMS-354825), on human prostate cancer cells, *Cancer Research* **2005**, *65*, 9185-9189.
[70] Evans, C. P.; Lara Jr, P. N.; Kung, H.; Yang, J. C. Activity of the Src-kinase inhibitor AZD0530 in androgen-independent prostate cancer (AIPC): pre-clinical rationale for a phase II trial, *Journal of Clinical Oncology* **2006**, *24*, 14542.
[71] Trevino, J. G.; Summy, J. M.; Lesslie, D. P.; Parikh, N. U.; Hong, D. S.; Lee, F. Y.; Donato, N. J.; Abbruzzese, J. L.; Baker, C. H.; Gallick, G. E.

Inhibition of SRC expression and activity inhibits tumor progression and metastasis of human pancreatic adenocarcinoma cells in an orthotopic nude mouse model, *The American Journal of Pathology* **2006**, *168*, 962-972.

[72] Gaur, P.; Samuel, S.; Bose, D. *et al.* Blockade of in vivo tumor growth of newly established human midgut carcinoid tumors by Src inhibition. *ASCO Gastrointestinal Cancers Symposium* **2009,** *146.*

[73] Araujo, J.; Logothetis, C. Dasatinib: a potent SRC inhibitor in clinical development for the treatment of solid tumors, *Cancer Treatment Reviews* **2010**, *36*, 492-500.

[74] Lu, Y.; Li, X.; Liang, K.; Luwor, R.; Siddik, Z. H.; Mills, G. B.; Mendelsohn, J.; Fan, Z. Epidermal growth factor receptor (EGFR) ubiquitination as a mechanism of acquired resistance escaping treatment by the anti-EGFR monoclonal antibody cetuximab, *Cancer Research* **2007**, *67*, 8240-8247.

[75] Wheeler, D. L.; Iida, M.; Kruser, T. J.; Nechrebecki, M. M.; Dunn, E. F.; Armstrong, E. A.; Huang, S.; Harari, P. M. Epidermal growth factor receptor cooperates with Src family kinases in acquired resistance to cetuximab, *Cancer Biology & Therapy* **2009**, *8*, 696-703.

[76] Price, C. M. Fluorescence in situ hybridization, *Blood Reviews* **1993**, *7*, 127-134.

[77] Bayani, J.; Squire, J. A. Traditional banding of chromosomes for cytogenetic analysis. *Current Protocols in Cell Biology* **2004**, *22.*

[78] Trask, B. J. Fluorescence in situ hybridization: applications in cytogenetics and gene mapping, *Trends in Genetics* **1991**, *7*, 149-154.

[79] Ramos-Vara, J. A.; Miller, M. A. When tissue antigens and antibodies get along: revisiting the technical aspects of immunohistochemistry - The red, brown, and blue technique, *Veterinary Pathology Online* **2014**, *51*, 42-87.

[80] Dabbs, D. J. *Diagnostic Immunohistochemistry. Theranostic and Genomic Applications, 4th edition*. Elsevier Saunders, Philadelphia **2013**.

[81] Painter, J. T.; Clayton, N. P.; Herbert, R. A. Useful immunohistochemical markers of tumor differentiation, *Toxicologic Pathology* **2010**, *38*, 131-141.

[82] Wintzer, H. O.; Zipfel, I.; Schulte-Mönting, J.; Hellerich, U.; Von Kleist, S. Ki-67 immunostaining in human breast tumors and its relationship to prognosis, *Cancer* **1991**, *67*, 421-428.

[83] Mooy, C. M.; Luyten, G.; De Jong, P.; Luider, T. M.; Stijnen, T.; Van de Ham, F.; Van Vroonhoven, C.; Bosman, F. T. Immunohistochemical and prognostic analysis of apoptosis and proliferation in uveal melanoma, *The American Journal of Pathology* **1995**, *147*, 1097.

[84] Skoog, L.; Tani, E. Immunocytochemistry: an indispensable technique in routine cytology, *Cytopathology* **2011**, *22*, 215-229.

[85] Jeng, Y.-M.; Peng, S.-Y.; Lin, C.-Y.; Hsu, H.-C. Overexpression and amplification of Aurora-A in hepatocellular carcinoma, *Clinical Cancer Research* **2004**, *10*, 2065-2071.

[86] Gritsko, T. M.; Coppola, D.; Paciga, J. E.; Yang, L.; Sun, M.; Shelley, S. A.; Fiorica, J. V.; Nicosia, S. V.; Cheng, J. Q. Activation and

overexpression of centrosome kinase BTAK/Aurora-A in human ovarian cancer, *Clinical Cancer Research* **2003**, *9*, 1420-1426.

[87] Klein, A.; Flügel, D.; Kietzmann, T. Transcriptional regulation of serine/threonine kinase-15 (STK15) expression by hypoxia and HIF-1, *Molecular Biology of the Cell* **2008**, *19*, 3667-3675.

[88] Hung, L.-Y.; Tseng, J. T.; Lee, Y.-C.; Xia, W.; Wang, Y.-N.; Wu, M.-L.; Chuang, Y.-H.; Lai, C.-H.; Chang, W.-C. Nuclear epidermal growth factor receptor (EGFR) interacts with signal transducer and activator of transcription 5 (STAT5) in activating Aurora-A gene expression, *Nucleic Acids Research* **2008**, *36*, 4337-4351.

[89] Lai, C. H.; Tseng, J. T.; Lee, Y. C.; Chen, Y. J.; Lee, J. C.; Lin, B. W.; Huang, T. C.; Liu, Y. W.; Leu, T. H.; Liu, Y. W.; Chen, Y. P.; Chang, W. C.; Hung, L. Y. Translational up-regulation of Aurora-A in EGFR-overexpressed cancer, *Journal of Cellular and Molecular Medicine* **2010**, *14*, 1520-1531.

[90] Summy, J. M.; Gallick, G. E. Treatment for advanced tumors: Src reclaims center stage, *Clinical Cancer Research* **2006**, *12*, 1398-1401.

[91] Dehm, S. M.; Bonham, K. SRC gene expression in human cancer: the role of transcriptional activation, *Biochemistry and Cell Biology* **2004**, *82*, 263-274.

[92] Tan, M.; Li, P.; Klos, K. S.; Lu, J.; Lan, K.-H.; Nagata, Y.; Fang, D.; Jing, T.; Yu, D. ErbB2 promotes Src synthesis and stability: novel mechanisms of Src activation that confer breast cancer metastasis, *Cancer Research* **2005**, *65*, 1858-1867.

[93] Biscardi, J. S.; Belsches, A. P.; Parsons, S. J. Characterization of human epidermal growth factor receptor and c-Src interactions in human breast tumor cells, *Molecular Carcinogenesis* **1998**, *21*, 261-272.

[94] Modlin, I. M.; Drozdov, I.; Kidd, M. The identification of gut neuroendocrine tumor disease by multiple synchronous transcript analysis in blood, *Plos One* **2013**, *8*, e63364.

[95] Ratushny, V.; Pathak, H. B.; Beeharry, N.; Tikhmyanova, N.; Xiao, F.; Li, T.; Litwin, S.; Connolly, D. C.; Yen, T. J.; Weiner, L. M.; Godwin, A. K.; Golemis, E.A. Dual inhibition of SRC and Aurora kinases induces postmitotic attachment defects and cell death, *Oncogene* **2012**, *31*, 1217-1227.

8. Erklärung zum Eigenanteil der Dissertationsschrift

Die Arbeit wurde im Institut für Pathologie und Neuropathologie des Universitätsklinikums Tübingen unter Betreuung von Prof. Dr. Bence Sipos durchgeführt.

Die Konzeption der Studie erfolgte durch Prof. Dr. Bence Sipos.

Sämtliche Experimente (Immunhistochemie, FISH) wurden von mir eigenständig durchgeführt. Die Anfertigung der TMAs erfolgte durch Dr. Maike Nieser und Christine Beschorner. Im Rahmen der Immunhistochemie und der Fluoreszenz *in situ* Hybridisierung wurden die Gewebeschnitte nach Einarbeitung durch Dr. Maike Nieser mit Unterstützung von Dennis Thiele von mir vorbereitet und analysiert. Die abgebildeten Mikroskop-Aufnahmen erfolgten mit Unterstützung von Prof. Dr. Bence Sipos und Dr. Maike Nieser.

Die statistische Auswertung erfolgte eigenständig mit Hilfe von Dr. Maike Nieser.

Ich versichere, das Manuskript selbstständig verfasst zu haben und keine weiteren als die von mir angegebenen Quellen verwendet zu haben.

Tübingen, den 15.01.2018

Paulina Kalmutzki

Acknowledgements

First, I would like to express my gratitude to my supervisor Prof. Dr. Bence Sipos for the opportunity to study this exciting field and to work in such a motivating environment. I am deeply grateful for his great mentorship and support at any time.

Furthermore, I sincerely thank Dr. Maike Nieser for her encouraging and supportive advice, intense teaching and guidance in laboratory work, assistance with statistical analysis of data and proofreading.

I would also like to thank Barbara Mankel for the opportunity to work in the FISH laboratory and to use the fluorescence microscope.

I am very thankful for the exceptionally friendly atmosphere within the research group and especially for working with Dennis Thiele, Karen Greif and Christine Beschorner who shared their valuable knowledge and experience with me.

Finally, I warmly thank my family and friends who helped me finish my dissertation. Most importantly, I am extremely grateful to my parents for their constant encouragement and patience during my studies. Special thanks to Markus for inspiring my interest in science and for the motivational support. Last but not least, thanks to Verena for making the years of study so much better.